RESEARCH ARTICLE

Pelagic ecosystem dynamics between late autumn and the post spring bloom in a sub-Arctic fjord

E. Zoe Walker[1,2,*], Ingrid Wiedmann[1], Anna Nikolopoulos[3], Jofrid Skarðhamar[3], Elizabeth M. Jones[3], and Angelika H. H. Renner[3]

Marine ecosystems, and particularly fjords, are experiencing an increasing level of human activity on a year-round basis, including the poorly studied winter period. To improve the knowledge base for environmentally sustainable management in all seasons, this study provides hydrographic and biological baseline data for the sub-Arctic fjord Kaldfjorden, Northern Norway (69.7° N, 18.7° E), between autumn 2017 and spring 2018. Field observations are integrated with results of a numerical ocean model simulation, illustrating how pelagic biomass, represented by chlorophyll a (Chl a), particulate organic carbon (POC), and zooplankton, is affected by stratification and circulation from October to May. We observed an unusually warm autumn that likely delayed the onset of cooling and may have supported the high abundances of holoplankton and meroplankton (5768 individuals m^{-3}). With the onset of winter, the water column cooled and became vertically mixed, while suspended Chl a concentrations declined rapidly (< 0.12 mg Chl a m^{-3}). In January and February, suspended POC concentrations and downward flux were elevated near the seafloor. The hydrodynamic model results indicate that the strongest currents at depth occurred in these months, potentially inducing resuspension events close to the seafloor. In spring (April), peak abundances of suspended biomass were observed (6.9–7.2 mg Chl a m^{-3} at 5–15 m; 9952 zooplankton ind. m^{-3} at 0–100 m), and field observations and model results suggest that zooplankton of Atlantic origin were probably advected into Kaldfjorden. During all investigated seasons, the model simulation suggests a complex circulation pattern, even in such a small fjord, which can have implications for environmental management of the fjord. We conclude that the pelagic system in Kaldfjorden changes continually from autumn to spring and that winter must be seen as a dynamic period, not a season where the fjord ecosystem is 'at rest'.

Keywords: Downward carbon flux, Seasonality, Winter ecology, Sub-Arctic fjord, Hydrography, Chlorophyll a, Zooplankton

Introduction

Estuaries, and in particular fjords, are productive ecosystems (Cloern et al., 2014; Valiela, 2015) used by various fish and marine mammals as feeding and breeding grounds (Falk-Petersen, 1982; Barthel et al., 1995; Similä et al., 1996; Viddi et al., 2010) and by humans for fishing, aquaculture, and recreation. To ensure that these ecosystem services persist in the future, sustainable management rooted in a sound understanding of the seasonal dynamics of lower trophic levels and the underlying hydrographic drivers is needed. While fjord system studies have been conducted for years during the productive spring and summer (e.g., Hegseth et al., 1995; Leu et al., 2011; Meire et al., 2016), winter has been

regarded as a period when high latitude ecosystems are "shut down" (Ross et al., 1993). Recent studies have challenged this view (Darnis et al., 2012; Berge et al., 2015a; Berge et al., 2015b, Coguiec et al., 2021), but pelagic fjord ecosystem dynamics and their hydrographic drivers throughout autumn, winter, and spring are still poorly understood.

In high latitudes, seasonal variability in environmental drivers such as light, temperature, and terrestrial runoff is enhanced compared to lower latitudes, and sub-Arctic fjords thus experience pronounced seasonality. Despite the highly variable meteorological and hydrographic conditions, many species inhabit fjords throughout the year. After the long winter darkness, the day length quickly increases, triggering a phytoplankton spring bloom sometime between March and May (Zenkevitch, 1963; Leu et al., 2011; Friedland et al., 2016). Subsequent to the bloom, zooplankton becomes more abundant and utilizes the accumulated autotrophic biomass (top-down control), which, in combination with the declining surface nutrient concentrations (bottom-up forcing), causes a reduction of

[1] UiT The Arctic University of Norway, Tromsø, Norway

[2] University Centre of the Westfjords, University of Akureyri, Ísafjörður, Iceland

[3] Institute of Marine Research, Tromsø, Norway

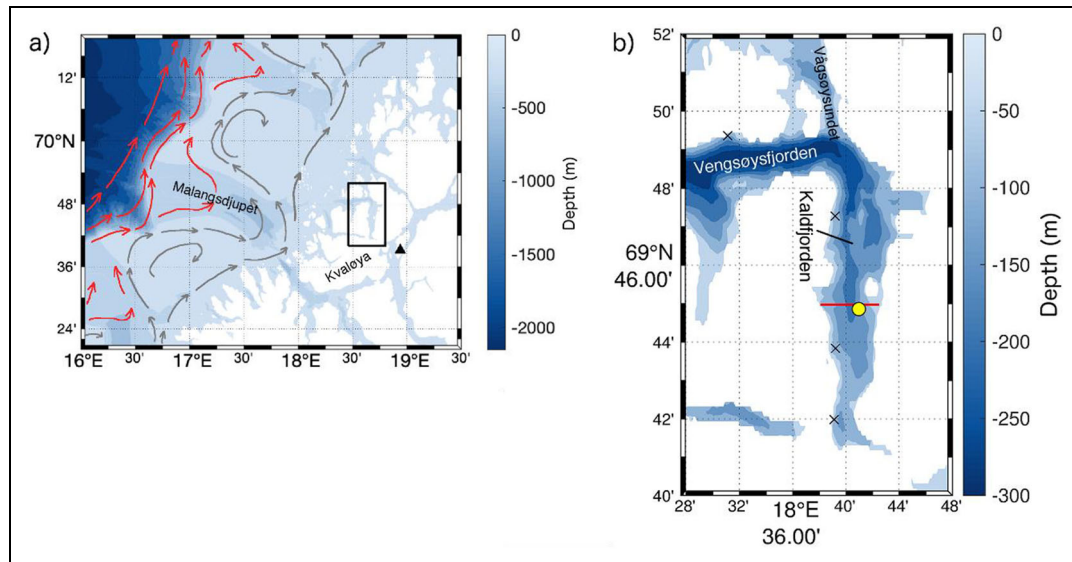* Corresponding author:
Email: zwyukon@gmail.com

Figure 1. Map of the study region in Northern Norway. (a) Bathymetric map of the shelf off Kvaløya, including Kaldfjorden (black rectangle). The black triangle denotes the position of the nearest weather station (Tromsø observation site). Grey arrows indicate the Norwegian Coastal Current, and red arrows the Norwegian Atlantic Current (after Sundby, 1984). (b) Detailed map of Kaldfjorden. The yellow marker shows the location of sampling station KaF. Black crosses indicate the locations of aquaculture pens. The red line indicates the transect used for volume flux calculations. In both maps, blue shading indicates bottom depth, land is shaded white. Depth data were obtained from the Norwegian Mapping Authority (2022). DOI: https://doi.org/10.1525/elementa.2021.00070.f1

the algal biomass in the euphotic zone during summer (Eilertsen et al., 1981; Eilertsen and Taasen, 1984). Wind mixing during autumn often causes a replenishment of the nutrient concentrations in the surface layer and an autumn bloom may occur (Eilertsen et al., 1981; Eilertsen and Frantzen, 2007), but this biomass increase is usually brief, lasting from days to a few weeks. As winter darkness returns, accompanied by surface cooling, reduced river runoff, and intensified vertical mixing, primary production declines rapidly and subsequently the biomass of both autotrophs and zooplankton strongly decreases (Weslawski et al., 1991; Falkenhaug et al., 1997; Hop et al., 2002; Marquardt et al., 2016; Marquardt et al., 2019; Michelsen et al., 2017). Due to the low biomass concentrations during winter, this season has long been regarded as a period where the ecosystem is in "a resting state" (Berge et al., 2015a). Winter has also been considered as the period when the fjord ecosystem "prepares" for the next productive season as surface nutrient concentrations are replenished (Eilertsen and Taasen, 1984) and phytoplankton resting spores may be resuspended into the water column (Hegseth et al., 1995). However, recent observations from Canadian coastal regions (Darnis et al., 2012) and Kongsfjorden on Svalbard (Berge et al., 2015a) challenged this understanding, because some pelagic and benthic organisms, such as bivalves and meroplanktonic ctenophores and pteropods, have been found to actively feed and grow during the high Arctic winter (Berge et al., 2015a).

To build on this new understanding of fjord ecology during winter, we investigated the transition from autumn to winter to spring in the sub-Arctic fjord Kaldfjorden (69.7° N; **Figure 1**) in the period October 2017 to May 2018. Kaldfjorden is a typical sub-Arctic (AMAP, 2018), ice-free fjord with anthropogenic influence in Northern Norway and may therefore serve as a model area for other fjords. In our study, we assessed the hydrography, the suspended and exported auto- and heterotrophic biomass (chlorophyll *a*, particulate organic carbon and nitrogen), and the zooplankton composition and abundance from field observations. These data were then integrated with results of a hydrodynamic model (NorFjords160). We investigated how physical drivers affect the pelagic ecosystem and the pelagic-benthic coupling in autumn, winter, and spring. We provide baseline data of a sub-Arctic fjord ecosystem during the less studied winter season, which is important, because it improves the general understanding and informs management of such ecosystems.

Materials and methods
Study site
Kaldfjorden is a north–south oriented fjord, 15 km long and 2–3 km wide, on the island of Kvaløya in Northern Norway **(Figures 1** and S1). The fjord is deepest (230 m) in the outer part and becomes gradually shallower towards the fjord head. Kaldfjorden is connected to the shelf and the northeast Atlantic through Vengsøyfjorden (approximately 270 m deep, 3–4 km wide) and the shallower and narrower Vågsøysundet (approximately 90 m deep, 1 km wide). The bathymetry west of Vengsøyfjorden is complex with a bank area about 60 m deep acting as a sill, archipelagos of small islands and skerries, and an off-shore shelf sea consisting of shallow banks (typically 60–70 m) intersected by deep troughs (> 400 m; **Figure 1a**). The deepest connection between Vengsøyfjorden and the

offshore trough Malangsdjupet is a 100 m deep channel cutting through the bank area (**Figure 1a**).

On the shelf off Norway, Norwegian Coastal Water (NCW) is carried northwards by the buoyancy-driven Norwegian Coastal Current (S < 35; Helland-Hansen and Nansen, 1909; Sundby, 1984). Further offshore, and partly below the NCW, the Norwegian Atlantic Current carries warm and saline Atlantic Water (AW, S > 35; Helland-Hansen and Nansen, 1909; Sundby, 1984) along the shelf break (**Figure 1a**). The exchange between Kaldfjorden and these water masses depends on the seasonally varying extent of the NCW on the shelf and the prevailing wind conditions. In spring and summer the increased presence of freshwater on the shelf, both from local runoff sources and advected by the coastal current from the south, strengthens the stratification. The NCW spreads out over the shelf, typically occupying the upper 50 to 100 m (Sundby, 1976; 1984; Skarðhamar and Svendsen, 2005). The more saline AW is restricted to the deeper parts of Malangsdjupet. Widening and shallowing of the NCW due to prevailing northeasterly winds may allow intermittent inflow of AW onto the shelf and into Vengsøyfjorden and Kaldfjorden (A Nikolopoulos, personal communication). During winter, stratification is weaker, the extent of NCW on the shelf is typically narrower and deeper (down to 200 m) than in summer (Sundby, 1976; 1984; Skarðhamar and Svendsen, 2005), and the predominantly southwesterly winds tend to force coastal water into Kaldfjorden. Kaldfjorden also experiences seasonal freshwater input through minor rivers during spring snowmelt and after substantial precipitation events, but its drainage area is rather small and not monitored (NVE Atlas, 2021).

Three sets of Atlantic salmon aquaculture pens are licensed in Kaldfjorden and one in Vengsøyfjorden with a total capacity for 1890 tons of fish in 2018 (**Figure 1b**; Norwegian Directorate of Fisheries, 2021). The innermost aquaculture site was not used during our study period in winter 2017–2018.

Hydrographic and meteorological measurements

We conducted monthly sampling at station KaF (69.746° N, 18.683° E, 130 m; **Figure 1b**) between October 2017 and May 2018 (**Table 1**). KaF is located above sloping topography on the eastern side of Kaldfjorden, east of the deep basin extending into this part of the fjord and south of Fiskøya, an island influencing the circulation in the fjord. As described by Kutti et al. (2007), particles originating from aquaculture activities are most likely to spread in the main current direction which in the case of Kaldfjorden is oriented north–south. Combined with the observation that the majority of particles sink to the seafloor close to the farm and supported by backscatter analyses from Acoustic Doppler Current Profilers (ADCPs) deployed on nearby moorings (Blom, 2021), measurements at KaF are unlikely to be affected by the nearby aquaculture pens.

Vertical profiles of conductivity, temperature, and depth (CTD) were taken using a SAIV SD208 CTD sensor (1 Hz sampling frequency), apart from December 2017 when a Seabird Electronics SBE911plus (24 Hz sampling

frequency) was used (**Table 1**). When deployed from small boats (vessels *Chinga* and *Dytiscus*; **Table 1**), the SAIV CTD was lowered and pulled up by hand or with a small winch, while a fast-mounted winch was used on larger vessels. Calibration samples for salinity were taken using a single 3-L Niskin bottle mounted on the rope above the SAIV CTD on small boats or using a CTD rosette with 12 Niskin bottles onboard R/V *Helmer Hanssen* (in April 2018). The salinity samples were analysed using a Guildline Portasal salinometer at UiT The Arctic University of Norway, and the resulting values were used for calibration of the SAIV conductivity measurements. As the occasionally used SBE CTDs are factory-calibrated annually and also calibrated against salinity samples throughout the year, we validated the SAIV CTD profiles with simultaneously obtained SBE CTD data when possible. For all CTD measurements, the downcast was extracted, in situ temperature was converted to potential temperature θ, and measurements were averaged (median) into 2-dbar depth bins. Potential density anomaly σ_θ was calculated referenced to surface pressure (0 dbar). Additional CTD measurements from the neighbouring fjord Malangen (Figure S1) for the period August 2017 to February 2018 were obtained from the project "Monitoring of the marine environment (Havmiljødata)" at UiT The Arctic University of Norway (see Mankettikkara, 2013, for details of data collection and processing).

Meteorological data for the study period were obtained from the Norwegian Meteorological Institute (2018). Air temperature, wind speed and direction, and precipitation recorded at the Tromsø observation site, approximately 14 km southeast of KaF, were used because it is the official weather observation site closest to Kaldfjorden (**Figure 1a**). Although wind data can vary considerably on small spatial scales due to orographic steering effects, wind measurements on Tromsø Island were presumed to represent the wind conditions in Kaldfjorden well, because both locations experience a similar north–south orientation with the surrounding mountains (Jones et al., 2020).

Hydrographic model data

Supporting information on hydrography and circulation in Kaldfjorden was obtained from the numerical NorFjords160 model which is based on the Regional Ocean Modelling System (ROMS; Shchepetkin and McWilliams, 2005; Haidvogel et al., 2008). The simulation used 35 vertical s-levels with enhanced resolution in the upper 50 m and a horizontal grid resolution of 160 m x 160 m covering the coast and fjords in Troms County. Forcing along the open boundaries was taken from the 800 m x 800 m NorKyst800 model (Albretsen et al., 2011; Asplin et al., 2020) that covers the entire Norwegian coast and is run operationally at the Norwegian Meteorological Institute (2019). Atmospheric forcing was provided by the Meteorological Co-operation on Operational Numerical Weather Prediction (AROME-MetCoOp; Müller et al., 2017), tidal forcing was imposed based on the global inverse barotropic model of ocean tides (TPXO7.2; Egbert and Erofeeva, 2002), and river runoff was incorporated using daily discharge data provided by the Norwegian

Table 1. Sampling schedule for pelagic sampling and sediment trap deployment at station KaF. DOI: https://doi.org/10.1525/elementa.2021.00070.t1

Nominal month	Date (dd.mm.yy)	Vessel[a]	CTD sensor[b]	Nutrient sampling[c] depths (m)	Suspended biomass[c] sampling depths (m)	Zooplankton haul depth ranges (m)	Sediment trap deployments[c] Depth (m)	Duration (h: min)
October	05.10.17	1	SAIV	0, 50, 100, 150, 174	5, 15, 30, 90	—[d]	20, 30, 50, 90	24:05
November	06.11.17	1	SAIV	0, 50, 100, 150, 159	5, 15, 30, 90	—	20, 30, 50, 90	24:50
	07.11.17	1	—	—	—	100–50, 50–0	—	—
December	01.12.17	2	SBE	2, 51, 101, 152, 166	5, 15, 30, 90	—	20, 30, 50, 90	24:20
	02.12.17	2	—	—	—	100–0	—	—
January	25.01.18	3	SAIV	0, 50, 100, 150, 167	5, 15, 30, 90	—	20, 30, 50, 90	25:00
	26.01.18	3	—	—	—	100–50, 50–0	—	—
February	15.02.18	3	SAIV	—	5, 15, 30, 90	—	20, 30, 50, 90	26:00
	16.02.18	3	—	—	—	100–50, 50–0	—	—
March	13.03.18	4	—	0, 50, 100, 150, 158	—	—	20, 30, 50, 90	24:08
	14.03.18	4	SAIV	—	5, 15, 30, 90	100–50, 50–0	—	—
April	04.04.18	5	SAIV	0, 50, 100, 151, 163	5, 15, 30, 90	100–50, 50–0	20, 30, 50, 90	25:30
May	22.05.18	3	SAIV	2, 55, 106, 154, 169	5, 15, 30, 90	—	20, 30, 50, 90	25:00
	23.05.18	3	—	—	—	100–50, 50–0	—	—

[a]Vessel specification: 1 indicates *Chinga*; 2, R/V *Johan Hjort*; 3, *Dytiscus*; 4, R/V *Johan Ruud*; 5, R/V *Helmer Hanssen*.

[b]SAIV indicates SAIV SD208; SBE, SBE911plus.

[c]All data were collected at station KaF, except nutrient data which were collected in proximity at 69.750° N, 18.680° E, 450 m from KaF in the deepest part of the fjord. Suspended biomass samples were analysed for chlorophyll *a* and particulate organic carbon and nitrogen; samples from the sediment trap cylinders were analysed for the downward flux of the same parameters.

[d]No observations.

Water Resources and Energy Directorate. The model performance has been evaluated in detail by Dalsøren et al. (2020), and the model has been applied in various biophysical studies in Norwegian fjords (e.g., Skarðhamar et al., 2018; Myksvoll et al., 2020; Carvajalino-Fernández et al., 2020). In Kaldfjorden, the model simulation was evaluated against hydrographic observations (temperature and salinity) taken monthly at three cross-fjord transects (Jones et al., 2020) and against current observations from two bottom-moored, upward-looking ADCP that were deployed about 3.7 km north and 1.5 km south of KaF, respectively; Blom, 2021). Temperature and salinity differences between the model and the observations were negligible and the hydrography is represented realistically both spatially and temporally. Modelled current velocities corresponded to the ADCP measurements with good agreement in speed and direction in the upper water column while slightly larger deviations occur close to the seafloor (A Nikolopoulos, personal communication).

To assess the circulation pattern in Kaldfjorden, hourly values of the modelled horizontal current velocities were extracted at depths of 10 and 90 m by linear vertical interpolation and assembled into monthly averages for October 2017 to May 2018. As a proxy for the occurrence of Atlantic-influenced water masses at the study site, the net volume flux of water with salinity S > 34 and potential density anomaly $\sigma_\theta > 27.0$ kg m^{-3} through an across-fjord transect at 69.75° N (18.635° E to 18.7082° E) was calculated from daily modelled fields between October 1, 2017, and May 31, 2018.

Nutrients, suspended biomass and sediment trap deployment

Water samples for inorganic nutrient analyses were collected at one station each in the inner (69.700° N, 18.660° E) and the outer part of Kaldfjorden (69.800° N, 18.670° E), as well as close to station KaF (69.750° N, 18.680° E; **Table 1**). These stations were located in the middle of the fjord, and thus allowed sampling of the deepest water layer. At the sampling station close to KaF, water for nutrient analysis was collected just below the surface, at approximately 50 m, 100 m, 150 m, and close to the bottom by repeated casts of a 3-L Niskin bottle. In the inner- and outermost station, the maximum sampling depth was adjusted to the fjord depths and at approximately 100 m and 201 m, respectively. From the Niskin bottle, water was transferred into 20-mL vials and preserved with chloroform and stored cool (4°C) until

analysis for NO_3^- plus NO_2^-, NO_2^- and $Si(OH)_2$ on a Flow Solution IV analyzer. Details of the analysis and as well as a detailed investigation of nutrient dynamics and carbonate chemistry in Kaldfjorden can be found in Jones et al. (2020).

Suspended biomass was collected in repeated casts of a 3-L Niskin bottle at 5 m, 15 m, 30 m, and 90 m at station KaF (**Figure 1b**). Subsequent to the water sampling, an anchored short-term sediment trap array was deployed at KaF with paired sediment traps (KC Denmark, inner diameter = 7.2 cm, 45 cm high) at 20, 30, 50, and 90 m for approximately 24 h (**Table 1**). A free-drifting sediment trap array would have allowed the determination of the downwards particle flux in a Lagrangian manner, but due to spatial restrictions in Kaldfjorden (15 km long, 2–3 km wide), at times strong winds (up to 7 m s^{-1} on daily average), and ship traffic (fishing vessels and leisure traffic) the trap array had to be moored. The deviation from the target depth of the sediment traps was $\pm$ 3.5 m (measured by a SCUBA diving computer attached to the 20-m sediment trap). The sediment trap cylinders were empty when lowered into the water and then filled with ambient water during the deployment. Downward particle flux determined in this way has previously been compared to the $^{234}Th/^{238}U$ disequilibrium method (Coppola et al., 2002) and found to be in good agreement. However, suspended biomass was assumed to flush into the sediment trap cylinder when it was filled with seawater (Persson, 2018). Therefore, we subtracted the suspended concentration of chlorophyll a (Chl a), particulate organic carbon (POC), and particulate organic nitrogen (PON) at the ambient depth of the sediment trap cylinder from the concentration of the respective parameter in the sediment trap cylinder. Based on the difference, the downward flux was calculated. We cannot distinguish if Chl a, POC or PON was transported into the sediment trap cylinder by gravitational sinking, the mixed-layer pump or a migrant pump (Boyd et al., 2019). To include all these processes, we use the term "downward (particle) flux" in the following to describe the transport of Chl a, POC, and PON from upper water layers to depth. Finally, the euphotic zone in North Norwegian fjords tends to extend down to 30–40 m in a pre-bloom phase and to 10–15 m in the bloom phase (Wassmann et al., 1996). We thus cannot exclude that the downward flux was overestimated at 20 m (March–May) and 30 m (March) due to weak primary production in the cylinder.

Water samples from the Niskin bottle and the sediment trap cylinders were transferred into carboys and stored dark and cool (> 0°C). Filtration was conducted within 6 h of sample collection, using a vacuum filtration system (−30 to −40 kPa). Triplicated subsamples of each carboy (200–400 mL; Table S1) were filtered onto Whatman GF/F filters (0.7 µm pore size) to determine the Chl a concentration and on pre-combusted GF/F filters (5 h at 450°C) for concentration of POC and PON. After filtration, all filters were frozen at −20°C. Within 2 months, the Chl a and phaeophytin concentration was determined by placing the filters overnight in 5 mL of methanol (in darkness, at 4°C) and subsequently measuring the Chl a concentration in the extract (Turner Design AU-10

Fluorometer calibrated with Chl a standard, Sigma S6144) following the acidification procedure (Holm-Hansen and Riemann, 1978). The concentration of POC and PON was determined within 4 months of sampling. After thawing, drying (24 h, 60°C) and removal of carbonates by HCl fumes (37% HCl, 24 h), the filters were analyzed in a Leeman Lab CHN Analyzer.

Zooplankton sampling and analysis

Zooplankton were sampled at KaF using a WP2 net (180-µm mesh size, 0.25-m^2 opening) following the procedures described in Daase and Eiane (2007). Two vertical tows (100–50 m and 50–0 m) were taken during each field period except for October (no zooplankton sampled) and December (one cast 100–0 m; **Table 1**). Each zooplankton sample (approximately 220 mL) was preserved with 25 mL of 36% formaldehyde solution buffered with 5 mg hexamethylenetetramine for laboratory analysis within 6 months of sampling. In the laboratory, the complete zooplankton sample was transferred into a beaker and diluted with 200–250 mL of tap water. Subsamples were inspected under a LEICA CLS 150X stereomicroscope and organisms < 2.5 mm were identified to the lowest possible taxonomic level (genus). Subsamples of 1–5 mL were counted until at least 300 individuals of the two most abundant species had been recorded. Due to very low abundances, the complete samples collected in January and February were analyzed for individuals < 2.5 mm. For organisms > 2.5 mm, the complete zooplankton samples were analyzed for all months and identified to the lowest possible taxonomic level (order or genus). Due to the mesh size of the WP2 (180 µm), nauplii and other small organisms (< 200 µm) must be assumed to be strongly undersampled (Nichols and Thompson, 1991). Definite numbers are therefore not presented here, but nauplii were found in each of the monthly zooplankton samples. Similarly, the first copepodite stages (CI–III) of small copepod species were likely undersampled (CI, up to 90% undersampling; CIII, up to 30%; Nichols and Thompson, 1991), which needs to be taken into account in the interpretation of the results. In addition, Coguiec et al. (2021) in nearby Ramfjorden (Figure S1) identified 4 times more zooplankton species by metabarcoding than by morphological identification alone, and as such we assume that the actual diversity at KaF is higher than indicated by our results.

Results

Meteorology

Air temperature in Tromsø follows a distinct seasonal cycle albeit with considerable variability. During our study period from September 2017 to the end of May 2018, the highest air temperatures were observed in May at > 15°C (**Figure 2a**). Lowest temperature was measured in March (−10°C) after a winter when cold periods (< −5°C) were interspersed with phases of temperatures > 0°C. Precipitation varied considerably throughout the study period. A very dry September in 2017 was followed by a wet autumn and early winter before another dry period occurred in mid-January to mid-March 2018 (**Figure 2b**). Wind
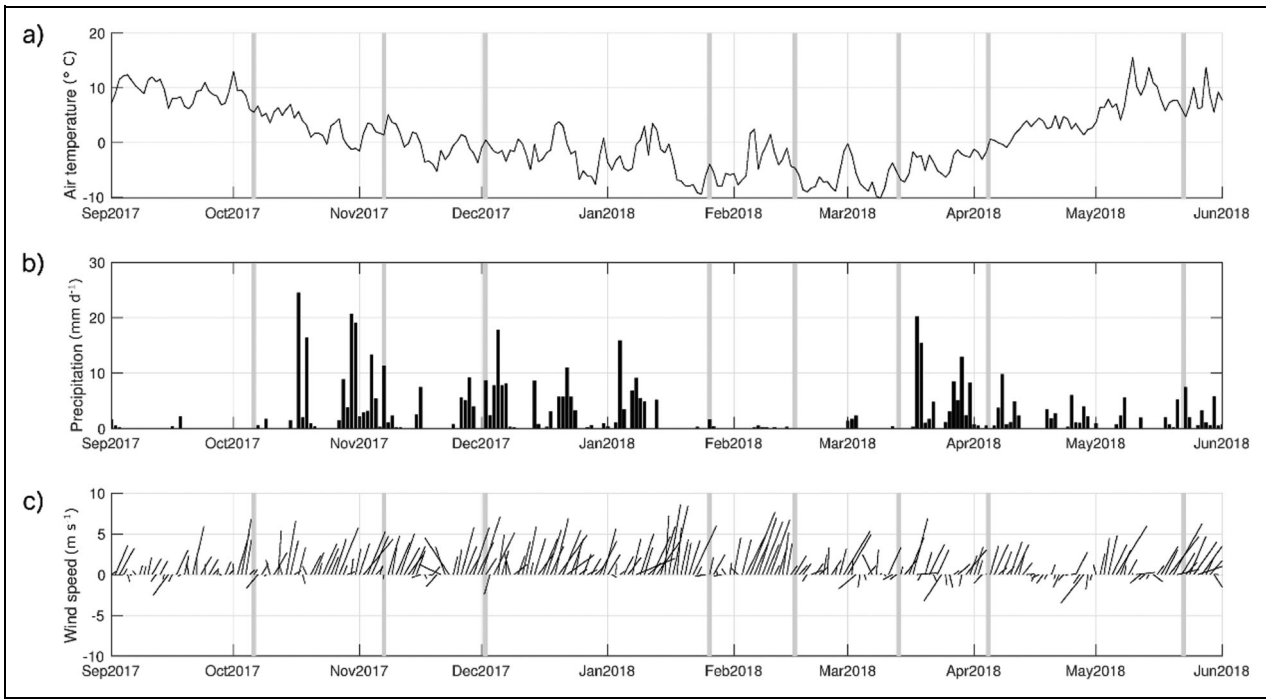
Figure 2. Meteorological observations at Tromsø observation site. (a) Daily average air temperature; (b) daily precipitation; (c) daily average wind vectors, where the vector orientation indicates the direction the wind is blowing towards. Grey vertical bars in all panels indicate the deployment periods of the sediment trap array. DOI: https://doi.org/10.1525/elementa.2021.00070.f2

conditions in Tromsø were dominated by south/south-westerly winds in autumn and winter, and more variable wind directions in spring and summer (**Figure 2c**). Very local cross-fjord winds caused by strong fall winds were also encountered at KaF during sampling in February and March but are not captured in the wind record.

Observed hydrography
In October 2017, the water column at KaF was stratified with a warm surface layer ($\theta = 9.6°C$) extending down to 70 m, and cooler and saline water (S > 34) occupying the deep layer (> 100 m; **Figure 3**). Decreasing air temperatures contributed to cooling of the surface waters during October and November (**Figures 2a** and **3a**). Increased precipitation probably enhanced the river run-off and, together with freshening of coastal water, resulted in surface freshening at KaF (**Figures 3b** and **4**). At the same time, autumn storms with high wind speeds (**Figure 2b**), together with the decreasing surface water temperatures, resulted in weakened water column stratification (**Figures 3a** and **4**). By January 2018, the water column was completely mixed as indicated by the close assemblage of data points in the temperature-salinity diagram (**Figure 4**) and continued to cool in February and March. Lowest temperatures were measured in the surface waters in April ($\theta = 2.5°C$), while the deep water layers were still > 3.4°C. Meanwhile, salinity at KaF increased from February to April (S = 33.4 to S = 33.89; **Figure 3b**). The increased spread in the data points in the temperature-salinity diagram (**Figure 4**) starting in March and continuing in April indicates that this increase was driven by inflow of more saline water at depth. In May, surface warming and increased river runoff during

snowmelt resulted in a re-established water column stratification with a thin warm and fresh surface layer ($\theta = 6.6°C$, S = 32.6) above the pycnocline and a cool and saline deep layer ($\theta = 3.5°C$, S > 33.5, **Figures 3** and **4**). Observations from nearby Malangen show a similar development from a warm and stratified water column in autumn to colder conditions in winter (Figure S2).

Modelled fjord circulation
For our study period, the Norfjords160 model results suggest a circulation pattern in the fjord with generally southward flow (corresponding to flow towards the fjord head) in the near-surface layer (10 m), with increased rotational activity in autumn and winter (**Figure 5a**). In January and February, the velocities at this depth were on average 0.02–0.03 m s^{-1} and 0.08–0.1 m s^{-1} at their maximum. In the other months, velocities were lower with a maximum speed of 0.03–0.06 m s^{-1}. The flow in the deeper layers (90 m) followed the bottom slope and was generally southward (towards the fjord head) along the western side and northward (towards the fjord mouth) along the eastern side of the fjord (**Figure 5b**). Currents were strongest during in January and February (on average 0.03–0.04 m s^{-1} and maximum 0.12 m s^{-1}), and in particular the northward current in the deep layer was intensified. An eddy-like feature was situated in the middle of the fjord with KaF on its eastern rim. This eddy was discernible throughout most of the year and most of the water column but enhanced during winter (**Figure 5**). Hence, northward currents persisted locally at KaF, although with varying strength throughout the seasonal cycle (**Figure 5a**). During January and February the northward flow at KaF
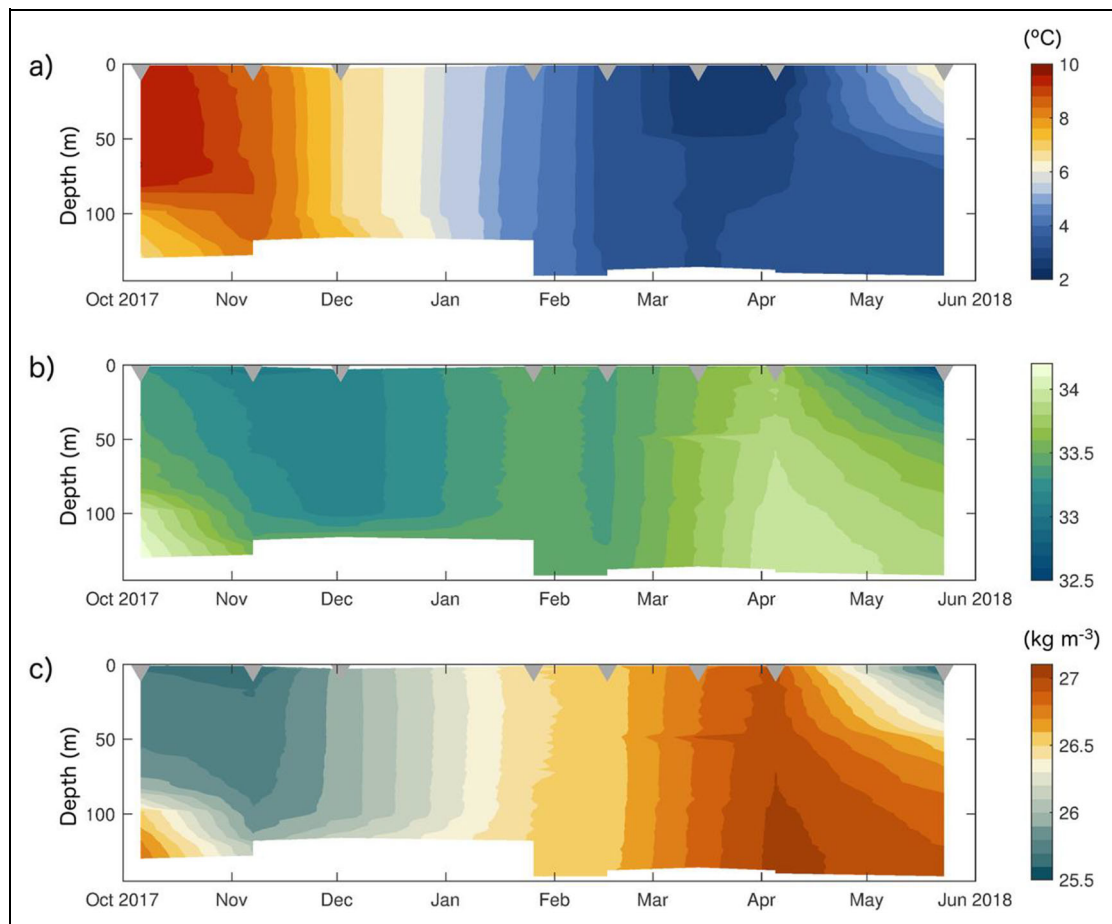
Figure 3. Hydrographic time series at KaF from October 2017 to late May 2018. Panels show (a) potential temperature, (b) practical salinity, and (c) potential density anomaly σ_θ. Grey triangles along the top axis of each panel mark the field campaigns in each month. DOI: https://doi.org/10.1525/elementa.2021.00070.f3

was 0.04–0.07 m s^{-1} at 10-m depth (0.06–0.1 m s^{-1} at 90-m depth), while it weakened to 0–0.03 m s^{1} (0.01–0.04 m s^{-1} at 90-m depth) in the remaining months.

The model results suggest that from March onwards, coastal and modified Atlantic Water (S > 34 and σ_θ > 27.0 kg m^{-3}) was advected into Kaldfjorden and reached station KaF (**Figure 6**). The inflow volume was largest in early spring and led to an increase in salinity first in the deep layers in the fjord (**Figure 4**).

Nutrient concentrations

The concentrations of nitrate and silicate at the sampling station close to KaF showed a typical high latitude seasonality (**Figure 7**). In October, nitrate was nearly depleted in the upper 50 m, but concentrations increased between October and late January to 5.4 µmol kg^{-1} (**Figure 7a**). The interpolation in **Figure 7a** suggests a steady decline in the surface nitrate between late January and mid-March, but we presume that this decline might be incorrect. As no nutrient samples are available from February, the surface nitrate concentration may also have remained high through most of February and rapidly declined in early March. From April onwards, nitrate in the upper 50 m was depleted (< 0.5 µmol kg^{-1}). Below 100 m, nitrate concentrations were > 1.6 µmol kg^{-1} throughout

most of the study period (apart from early October and early April; **Figure 7a**).

Low silicate concentrations were only observed at the surface in October 2017 (0.7 µmol kg^{-1}), while the rest of the year they were higher (0.8–5.1 µmol kg^{-1}). The highest concentrations were found close to the seafloor in early December. Unlike the nitrate concentration, silicate concentrations were still high (> 3.3 µmol kg^{-1}) throughout the whole water column in April (**Figure 7b**). Nutrient concentrations determined in the inner and outer part of Kaldfjorden (Figures S3 and S4) show that the seasonality described above took place not only close to KaF, but throughout Kaldfjorden.

Suspended biomass in the water column (Chl a and POC)

The Chl a and POC concentrations in the water column showed a clear seasonality in Kaldfjorden. During early October, elevated Chl a and POC concentrations were observed (0.09–3.15 mg Chl a m^{-3}, 82–315 mg POC m^{-3}; **Figure 8a** and **b**, Table S2), but they declined throughout autumn and were low from December to March (0.02–0.12 mg Chl a m^{-3}, 20–114 mg POC m^{-3}; **Figure 8c** and **d**). In winter, the C: N ratio of the suspended biomass at KaF had a wide range (6.56–13.48;

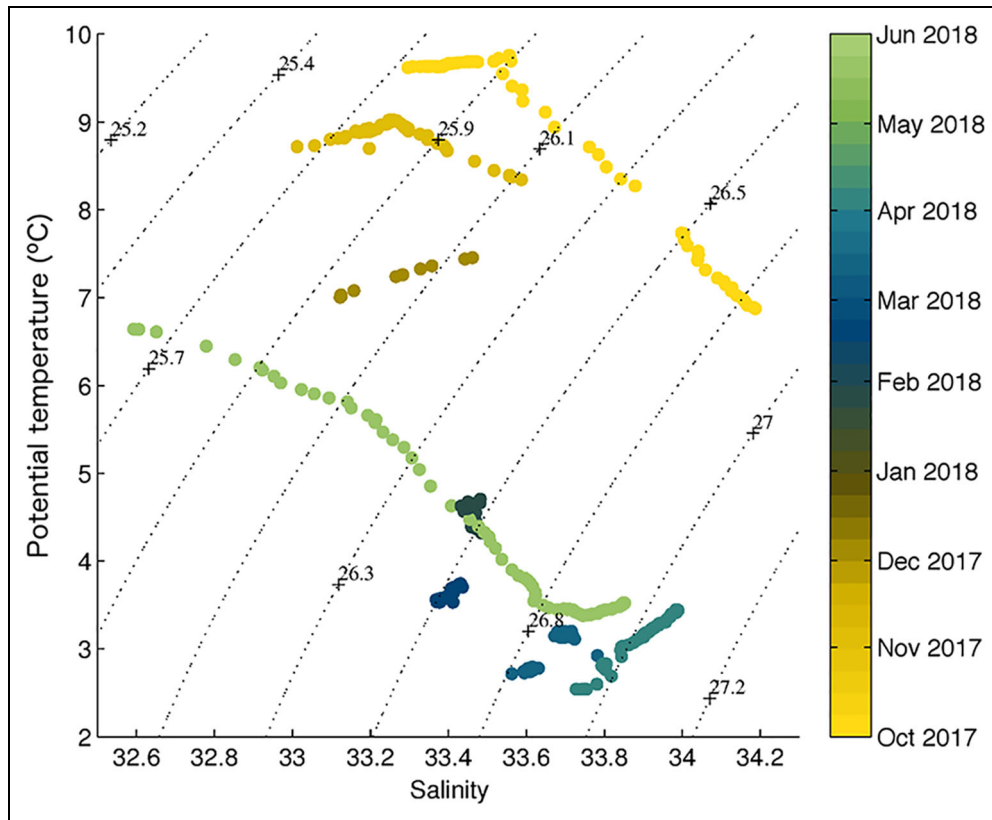**Figure 4. Temperature-salinity diagram from October 2017 (yellow) to late May 2018 (green).** Dotted lines indicate isopycnal contours. DOI: https://doi.org/10.1525/elementa.2021.00070.f4
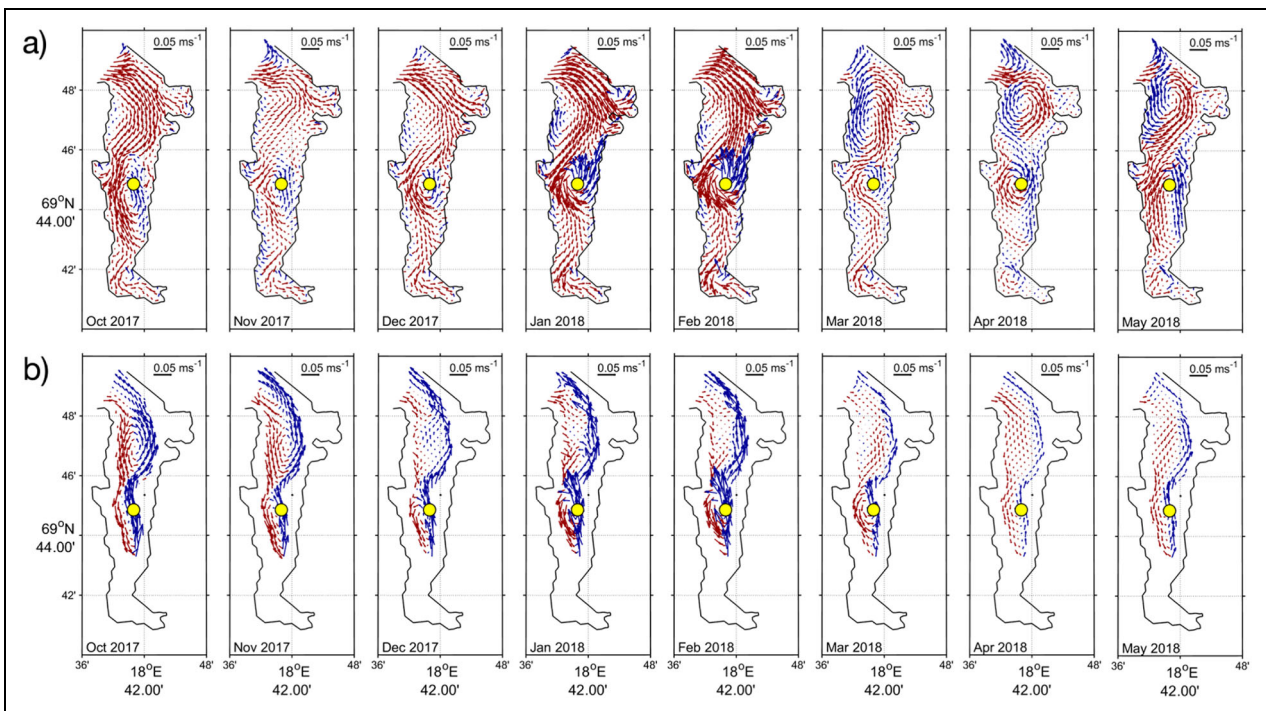
Figure 5. Monthly averaged velocity fields from the NorFjords160 model at (a) 10 m and (b) 90 m. Panels show October 2017 to May 2018 from left to right. Red and blue arrows show currents directed into and out of the fjord, respectively. The length of the arrows corresponds to current speed (reference arrow given in upper right corner). The yellow marker indicates the location of station KaF. DOI: https://doi.org/10.1525/elementa.2021.00070.f5
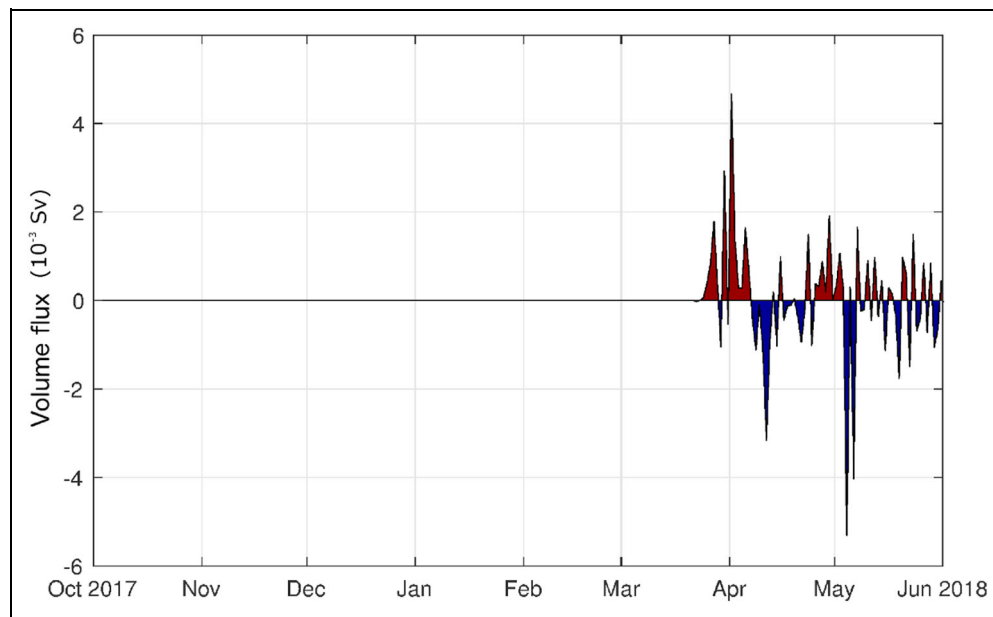
Figure 6. Net volume water transport with Atlantic Water signature across 69.75° N within Kaldfjorden (NorFjords160 model). Data shown between October 2017 and June 2018 with Atlantic Water signature defined as potential density anomaly > 27.0 kg m^{-3}, S > 34. Positive values shown in red indicate a net southward flow (i.e., into the fjord); negative values in blue show the inverse (i.e., out of the fjord), in correspondence with **Figure 5**. For the position of the transect see **Figure 1**. DOI: https://doi.org/10.1525/elementa.2021.00070.f6
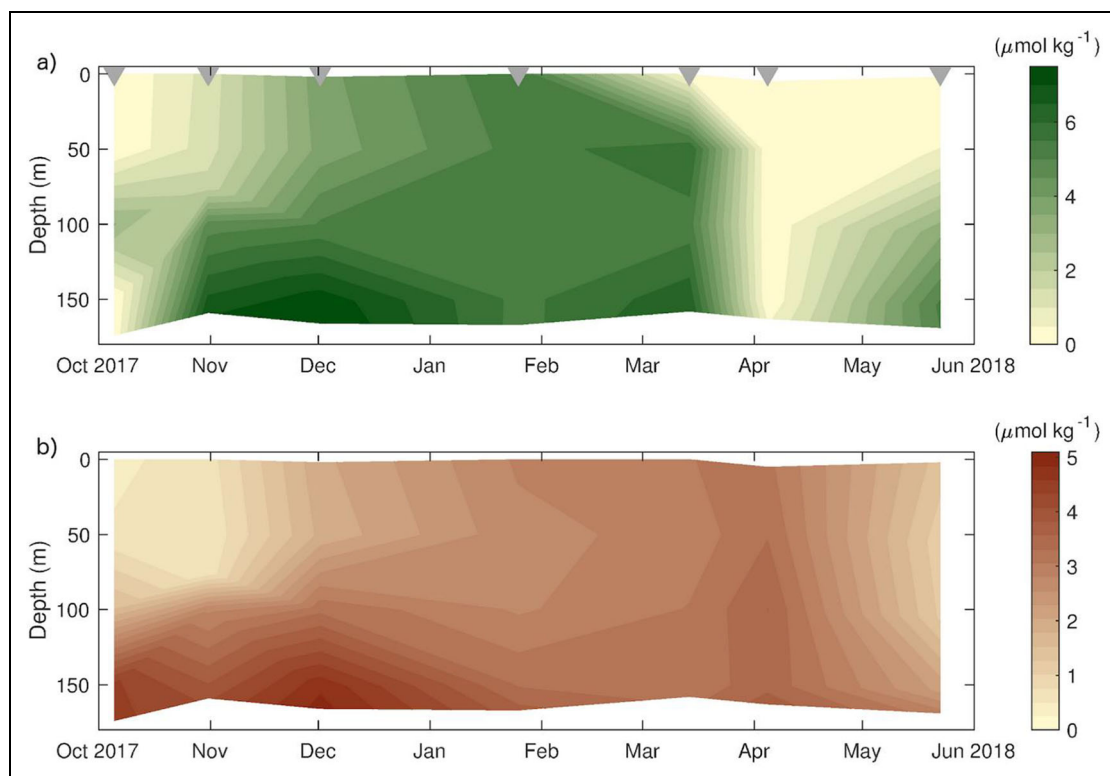

Figure 7. Nitrate (a) and silicate (b) concentrations close to KaF (October 2017 to May 2018). The top figure shows the seasonal variation of the nitrate (NO_3^-) concentration determined from water samples at subsurface, 50 m, 100 m, 150 m and close to the seafloor, while the bottom figure shows the silicate ($Si(OH)_2$) concentration determined from the same depths. The darker the color in the color scheme, the higher the concentration. Grey triangles along the top axis of each panel mark the time of the field campaign each month. DOI: https://doi.org/10.1525/elementa.2021.00070.f7
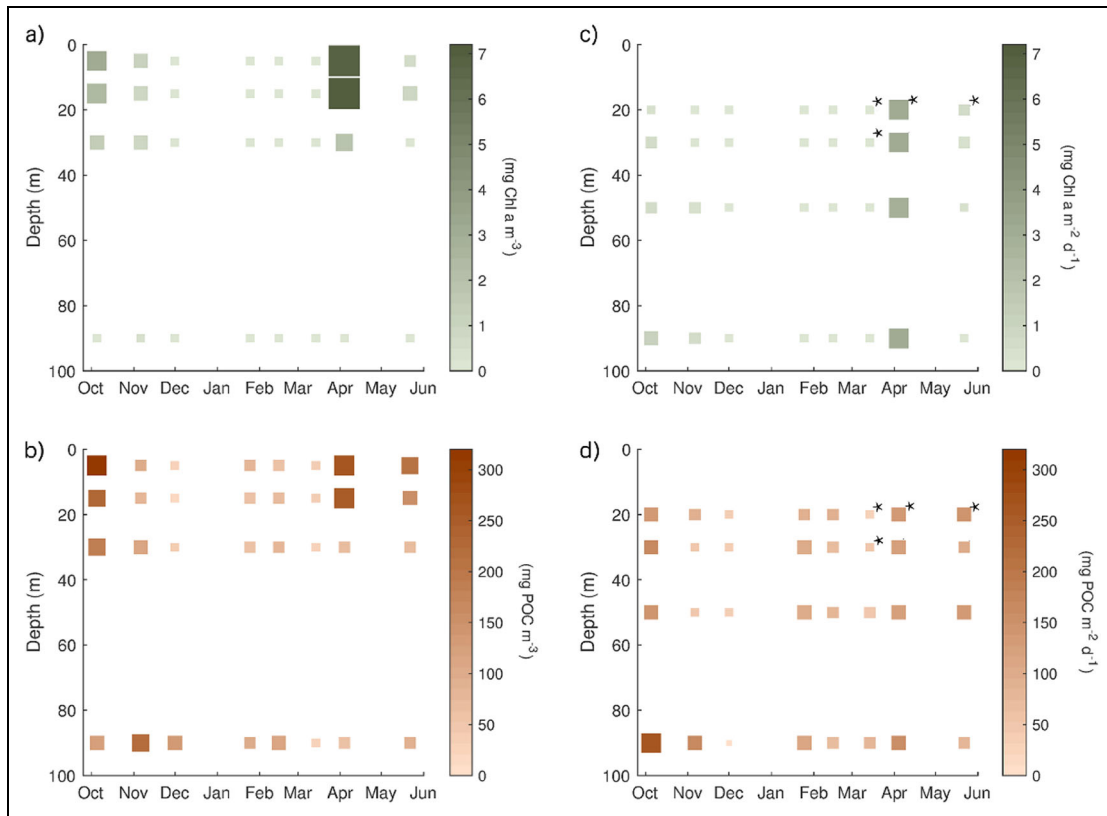
Figure 8. Suspended biomass (left) and downward flux (right) at KaF (October 2017 to May 2018). (a) Concentration of suspended chlorophyll a (mg Chl a m^{-3}), (b) concentration of suspended particulate organic carbon (mg POC m^{-3}), (c) downward flux of Chl a (mg Chl a m^{-2} d^{-1}), (d) downward flux of POC (mg POC m^{-2} d^{-1}). Colour and size of the squares indicate the magnitude of the variables, and detailed numbers can be found in the NMDC database (Walker and Wiedmann, 2022). The black stars mark sediment trap cylinders that were deployed at the transition of the euphotic to the aphotic zone, where a minor overestimation of the flux due to potential primary production cannot be excluded. DOI: https://doi.org/10.1525/elementa.2021.00070.f8

Table S2) as well as the POC: Chl a ratio (198–4031; Table S2) and indicates a mix of very degraded and carbon-rich material with somewhat less degraded biomass in the water column. The ratio of active Chl a to the sum of total photosynthetic pigments (Chl a + phaeophytin, Phaeo) was always < 0.7 (Table S2), and suggests a negligible amount of fresh autotrophic biomass during the polar night. In April, we observed high Chl a and POC concentrations in the water column (up to 7.2 mg Chl a m^{-3}, up to 264 mg POC m^{-3}; **Figure 8a** and **b**), a C: N ratio of approximately 6, a Chl a:(Chl a + Phaeo) ratio of 0.5–1.4, and a POC: Chl a ratio of 35–39 at 5–50 m (and 557 at 90 m). Despite the generally similar seasonal pattern, the suspended concentrations of Chl a and POC were not entirely synchronized throughout our study period. While the highest Chl a concentration was observed in the surface layers (5 and 15 m) in April (6.9–7.2 mg Chl a m^{-3}; **Figure 8a**), the highest POC concentration was found in October at 5 m (315 mg POC m^{-3}; **Figure 8b**). In addition, the Chl a concentration at 90 m was very low throughout the study period (< 0.3 mg Chl a m^{-3}; **Figure 8a**), while POC concentrations were always considerable at 90 m (30–216 mg POC m^{-3}; **Figure 8b**). In November, the POC concentration at 90 m even exceeded the POC concentrations in the surface layers.

Downward particle flux (Chl a and POC)

A seasonality was also observed in the downward flux of Chl a. It was low in October (0.3–1.1 mg Chl a m^{-2} d^{-1}; **Figure 8c**, Table S3), and declined to near-zero during winter (December to March: $\leq$ 0.10 mg Chl a m^{-2} d^{-1}; **Figure 8c**) with low Chl a:(Chl a + Phaeo) ratios (< 0.34) and high POC: Chl a ratios (519–2263, with one exception of 165; Table S3) at the four sampling depths. In April we observed the highest downward Chl a fluxes during this study (3.1 mg Chl a m^{-2} d^{-1} at 20 m and 30 m; **Figure 8c**), accompanied by the highest Chl a:(Chl a + Phaeo) ratio (0.5–0.6; Table S3), the lowest POC: Chl a ratios (37–51), and the lowest C: N ratios (6.2–6.8; Table S3) in the sinking material. Subsequent to the intense downward Chl a flux in April, the flux was low again in May and comparable to the Chl a flux in November. In contrast, seasonality in the POC flux was less clear (**Figure 8d**). The strongest downward POC flux was found at 90 m in October (259 mg POC m^{-2} d^{-1}; **Figure 8d**), with considerable POC fluxes also being measured at the other sampling depths in October (136–160 mg POC m^{-2} d^{-1}; **Figure 8d**). The lowest downward POC fluxes were in December and March (8–83 mg POC m^{-2} d^{-1}; **Figure 8d**), while intermediate fluxes were observed in April and May (85–157 mg POC m^{-2} d^{-1}; **Figure 8d**).
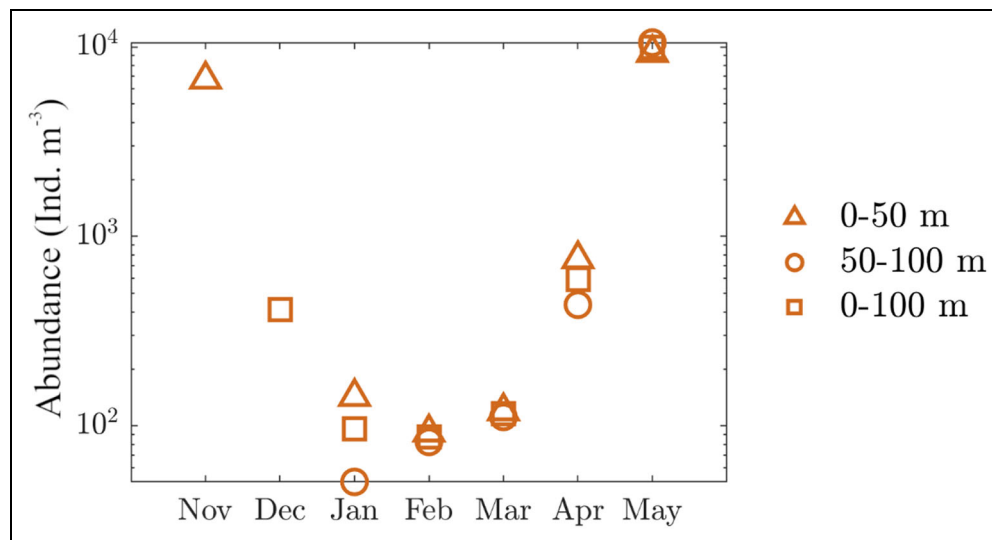
Figure 9. Total zooplankton abundance at station KaF. Zooplankton (holoplankton and meroplankton) was sampled with a WP2 of 180-µm mesh size, and total abundances are given by depth interval as the average number of individuals (ind.) m^{-3}. Note the logarithmic scale of the y-axis, and that the rather coarse mesh size of the WP2 may have resulted in some undersampling of taxa < 200 µm. DOI: https://doi.org/10.1525/elementa.2021.00070.f9

Zooplankton abundance and composition

At KaF, the total zooplankton abundance and composition varied considerably with season. In November (50–0 m), zooplankton was very abundant with 6808 individuals (ind.) m^{-3} (**Figure 9**), but then zooplankton abundance declined during winter (December to mid-March) when it was very low (97 ind. m^{-3} in January, 100–0 m; 87 ind. m^{-3} in February, 100-0 m; **Figure 9**). This seasonal trend was observed for both large copepods (**Figure 10a**), small copepods (**Figure 10b**), and meroplankton (**Figure 10c**). *Oithona* was the most abundant taxon in all winter months and at all sampling depths, except for March (50–0 m) when *Microcalanus* was observed more frequently (**Figure 10b**). The overall zooplankton abundance during spring (April and May) was distinctly higher (598 ind. m^{-3}) than in winter and dominated by meroplankton (537 ind. m^{-3}, 50–0 m), in particular by Cirripedia nauplii (287 ind. m^{-3}) and larvae of benthic Polychaeta (247 ind. m^{-3}). The highest total zooplankton abundance of this study occurred in May (9931 ind. m^{-3}, 100–0 m; **Figure 9**). Copepods with prosome length > 2.5 mm, especially *Calanus* spp. (7116 ind. m^{-3}, 100–0 m) and *Metridia* spp. (1382 ind. m^{-3}, 100–0 m) were also observed frequently (**Figures 9** and **10**, Table S4).

Discussion

Based on the meteorological data, the field observations in Kaldfjorden, and the numerical model results, we have divided the sampling period from October 2017 to May 2018 into three seasonal periods. In October and November, the water column cooled, the stratification weakened, and the suspended biomass of low trophic levels declined. The model results indicate that the general fjord circulation was dominated by inflow near the surface and outflow at depth. We characterize this period as *Late Autumn*.

Between December and mid-March, the water column was well mixed and very low concentrations of suspended biomass were found in the water column. We therefore classify these months as *Winter*. Finally, in April and May the daylight period was > 12 h per day and surface warming started, which led to the re-establishment of water column stratification. During this time with relatively low water velocities, the concentration of suspended Chl *a* peaked (April), and a maximum abundance of zooplankton followed in May. We refer to these months as *Spring*. In the following, we discuss the lower trophic ecosystem functioning in the high latitude Kaldfjorden during the autumn-to-spring transition. Finally, we elaborate on the implications of our findings for high latitude fjord systems which are important areas for marine life and industrial activities (e.g., aquaculture, tourism) during winter.

Late autumn (October to November)

During October, the water temperature at KaF (**Figure 3**) was > 9.6°C in the near-surface layer which is at the upper limit of the previously reported range from outer Malangen (69.5° N, 18.35° E, approximately 30 km south of KaF, 7–10°C; Mankettikkara, 2013). Hydrographic observations from Malangen (Figure S2) confirm these warmer-than-usual autumn conditions. We presume that this relatively warm water at KaF was a result of the high air temperature in September 2017 (**Figure 2a**). Little cloud cover and many hours of sunshine (www.eklima.no) likely resulted in the high Chl *a* and POC concentrations at KaF in October (at 5–30 m, 1.4–3.1 mg Chl *a* m^{-3}, 124–315 mg POC m^{-3}; **Figure 8a** and **b**, Table S2). These concentrations were higher than previous observations from other fjords in Northern Norway (Malange, < 1.3 mg Chl *a* m^{-3}; Wassmann et al., 1996; Altafjorden, 70.1° N, 23.2° E, 175 km northeast of KaF, < 2.2 mg Chl *a* m^{-3}; Eilertsen and
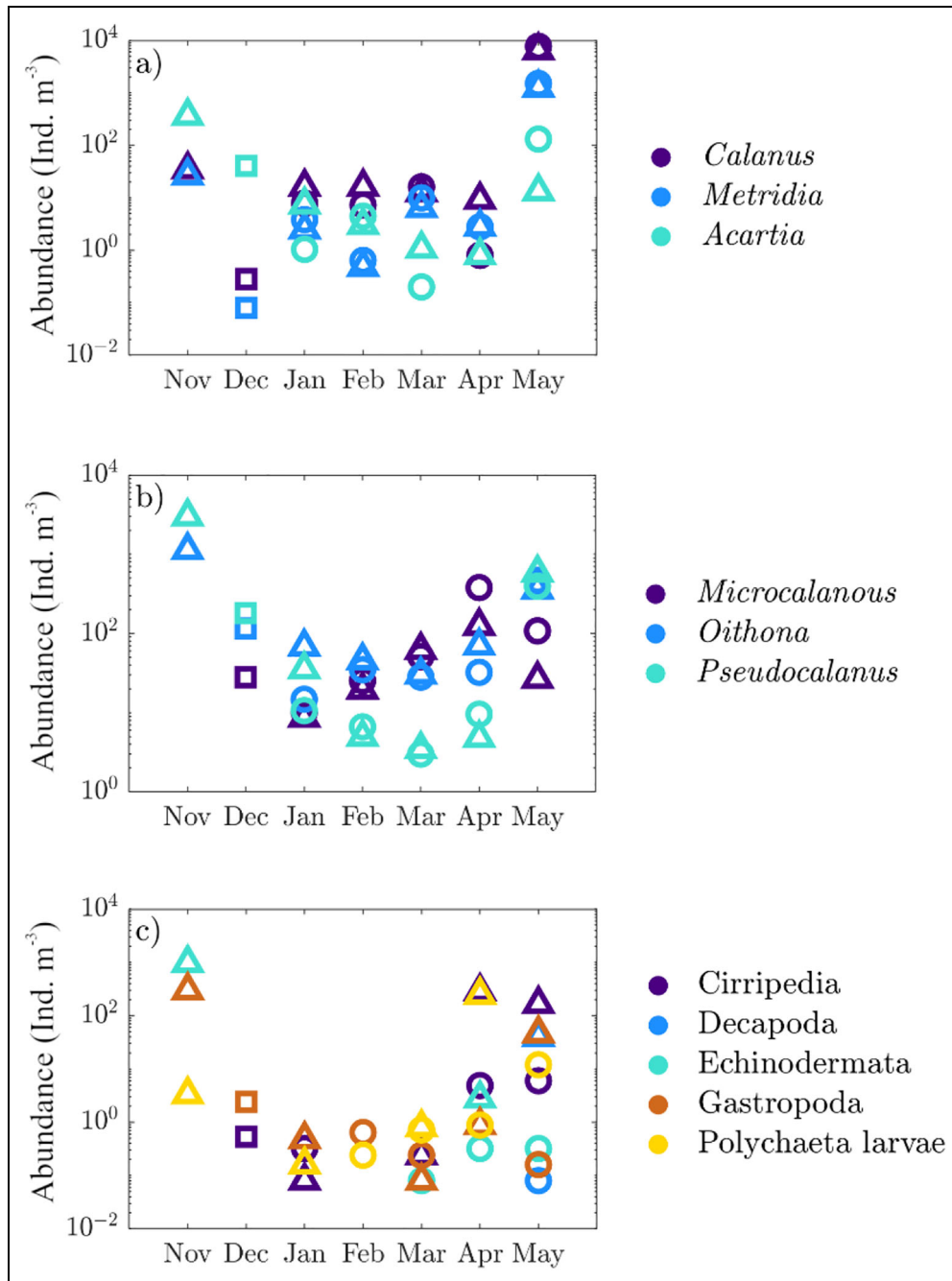
Figure 10. Zooplankton abundance between November 2017 and May 2018 at station KaF. Average abundance (in individuals (ind.) m^{-3}) of (a) the dominant large (> 2 mm prosome length) copepod taxa, (b) the dominant small copepod taxa (< 2 mm prosome length) and (c) of the most abundant meroplankton larvae in the depth layer 0–50 m (open triangles) and 50–100 m (open circles). Please note the logarithmic scale on the y-axis, the exceptions of the sampling scheme in November (only 0–50 m sample) and December (only one 0–100 m sample, shown as open squares), and that both small copepods and meroplankton larvae may have been undersampled due to the mesh size (180 µm) of the zooplankton net used. DOI: https://doi.org/10.1525/elementa.2021.00070.f10

Frantzen, 2007; Figure S1) and from Svalbard during autumn (0.1–0.4 mg Chl *a* m^{-3}; Zajączkowski et al., 2010; Wiedmann et al., 2016). We presume that the autotrophic biomass observed during autumn was freshly produced, because neither the C: N ratios (7.7–8.2; Table S2) nor the POC: Chl *a* ratios (95–135; Table S2) in the upper 50 m suggest the dominance of old, resuspended matter (Meyers, 1994; Barth et al., 1998; Engel et al., 2002).

However, the nutrient concentrations at the surface and 50 m imply that NO_3^- and NO_2^- were depleted in late summer and October (Table S2; Jones et al., 2020), and thus which nitrogen source fueled the Chl *a* production is unclear. Potential explanations are regenerated production using ammonium (no data available) or production based on nitrite (0.2 µg kg^{-1} at the surface < 1 km from KaF; Jones et al., 2020), but both explanations are highly

speculative. Between October and November, the Chl *a* and POC concentrations declined in the water column at KaF (**Figure 8a** and **b**), which has also been reported from nearby Ramfjorden (69.55° N, 19.12° E, about 30 km southeast of KaF; Noji et al., 1993; Figure S1). At the same time, the surface concentrations of nitrate and silicate increased (**Figure 7**), which was likely caused by a combination of increased vertical mixing and replenishment from higher concentrations at greater depth and diminished growth (and nutrient uptake) by phytoplankton. Additionally, the downward fluxes of Chl *a* and POC at KaF were lower in November than in October (**Figure 8c** and **d**). We hypothesize that the approaching polar night and the associated low Chl *a* and POC concentrations in the water column caused the weak downward flux, because little biomass remained in the water column to contribute to the flux in November.

The high number of zooplankton during November (average abundance in depth interval 0–50 m for meroplankton was 1280 ind. m^{-3}; for copepods, 4681 ind. m^{-3}; **Figure 9**) may have further reduced the downward biomass transport. Compared to other late autumn studies, the total abundance of copepods found at KaF was in the same order of magnitude as a study using a zooplankton net with the same mesh size (180 μm, approximately 1000 ind. m^{-3}) at Porsangerfjorden (70.5° N, 25.5° E, about 270 km northeast of KaF; Figure S1; Michelsen et al., 2017). However, our total zooplankton abundance was low compared to a study where a zooplankton net with a finer mesh size (85 μm; 76 347 ind. m^{-3}) was used at Porsangerfjorden (Priou, 2015). Data from the ADCP can be used to fill the gaps prior to and between our zooplankton samplings in Kaldfjorden. Both in October and November 2017, high backscatter indicated a substantial abundance of zooplankton conducting diel vertical migration (Blom, 2021). In addition to underestimating abundance, our species list also likely underestimates species diversity at KaF, because metabarcoding has been shown to produce a more comprehensive list of species in fjords (Coguiec et al., 2021). As this study is not a taxonomic study, we presume that our zooplankton data set (based on visual inspection and use of a 180 μm WP2 net) is sufficient for examining the transition of the fjord ecosystem from autumn to winter to summer.

The most abundant taxon at KaF, *Pseudocalanus* (approximately 3000 ind. m^{-3}), exceeded findings in Håkøybotn, a bay close to Kaldfjorden (Norrbin et al., 1990; Figure S1). However, the abundance of *Pseudocalanus* spp. is known to have high interannual variability (Norrbin, 1996), and Priou (2015) found similarly high numbers of *Pseudocalanus* spp. in Porsangerfjorden (Figure S1). Therefore, we consider the abundances reported here to be in an elevated but reasonable range. In Northern Norway and Svalbard, the *Pseudocalanus* species *P. acuspes* and *P. minutus* have been observed frequently (e.g., Barthel et al., 1995; Lischka and Hagen, 2005; Coguiec et al., 2021) and are presumed to be omnivorous (Norrbin, 1996). We therefore assume that the *Pseudocalanus* spp. observed at KaF belong to these species, though

genetic metabarcoding would be needed to confirm this assumption.

Oithona, the second most abundant taxon at KaF, has been observed in similar concentrations in fjords in Northern Norway and Svalbard (Falkenhaug et al., 1997; *O. similis* in Lischka and Hagen, 2005; Coguiec et al., 2021). *Oithona* predominantly feeds on phytoplankton (Pond and Ward, 2011; Zamora-Terol and Saiz, 2013), and protozooplankton (Nishibe et al., 2010), a feeding pattern that we expect sustained an abundant population into late autumn. However, the abundance of meroplankton (Echinodermata and Gastropoda) found in November exceeded previous findings of meroplankton in October by a factor of up to 25 (50 ind. m^{-3} at Porsangerfjorden, WP2 180 μm mesh size; Michelsen et al., 2017; 400 ind. m^{-3} on the shelf off Vesterålen, 69° N, WP2 200 μm mesh size; Silberberger et al., 2016; and 40–120 ind. m^{-3} at Balsfjorden, 69.36° N, 19.12° E, about 45 km southeast of KaF, WP2 150 μm mesh size; Falk-Petersen, 1982; Figure S1). Further, Falk-Petersen (1982), Silberberger et al. (2016), and Michelsen et al. (2017) reported Gastropoda and Bryozoa to be dominant in late autumn, while Echinodermata larvae dominated at KaF in November. As similar mesh sizes were used in these three studies, the under-sampling of the meroplankton was likely comparable between them. We therefore speculate that the warm weather and the still high Chl *a* concentrations in October may have resulted in the high numbers of echinoderm larvae at KaF, because sea surface temperature and food availability have previously been suggested to affect the abundances of these larvae (Kirby et al., 2008). In addition, the hydrographic observations and hydrodynamic model results indicate predominance of local and coastal water and reduced inflow of saline AW-derived water masses, which limits dilution of the local fjord waters and thus supports the high abundances of echinoderm larvae at KaF.

Winter (December to mid-March)
Between mid-December and mid-March, air temperatures were < 0°C in Tromsø (**Figure 2a**), causing surface cooling in Kaldfjorden. Minimum water temperatures were reached in mid-March (2.7°C at surface, 3.1°C at 94 m; **Figure 3a**), which is within the observed range in outer Malangen in the years 1930–2012 (2.0–5.5°C at surface, 3.0–7.8°C at 100 m; Mankettikkara, 2013) and during the study period (Figure S2a). Salinity at KaF increased throughout winter (**Figures 3b** and **4**), with a similar seasonality also reported from outer Malangen (Mankettikkara, 2013; Figure S2b). Following the changes in temperature and salinity throughout winter, the water column stratification and nutrient distribution also changed. In December and January, waters at KaF were still weakly stratified with a deep pycnocline at about 100 m. Thereafter a combination of winds (daily average speed of > 5 m s^{-1}; **Figure 2c**), surface cooling and convective mixing (**Figures 2a**, **3**, and **4**), and strong horizontal currents at all depths (**Figure 5**) resulted in a well-mixed water column at KaF during late winter (**Figures 3c** and **4**) and the replenishment of nitrate and silicate (**Figures 7**, S3, and S4).

Despite the enhanced nutrient concentrations, the cool, unstratified water column at KaF in combination with the low levels of incoming solar radiation during winter seemed to be an adverse environment for phytoplankton and zooplankton at KaF. The Chl a concentration declined abruptly between November and December and was near zero (< 0.12 mg Chl a m^{-3}) at KaF until March. Similar winter concentrations have been reported from fjords in Northern Norway and Svalbard (Weslawski et al., 1991; Noji et al., 1993; Eilertsen and Degerlund, 2010; Berge et al., 2015a). Moreover, these low suspended Chl a concentrations likely explained the negligible downward flux of Chl a during winter (**Figure 8c**), which resembled observations from Ramfjorden (Figure S1) during late November (Noji et al., 1993). At the end of winter, we suspect that even in a small fjord such as Kaldfjorden, the onset of the spring bloom may vary spatially. We presume that by mid-March, the spring bloom had already started in outer Kaldfjorden, because there the surface nutrient concentrations were already somewhat lower than during winter (Figure S4). At KaF, however, nutrient concentrations were still comparable to winter conditions (**Figure 7**).

Unlike the Chl a concentration, suspended POC concentrations at KaF were never near zero during winter (20–114 mg POC m^{-3}), though they were at the lower end of findings in Adventfjorden, Svalbard (43–143 mg POC m^{-3}; Wiedmann et al., 2016), Ramfjorden (70–160 mg POC m^{-3}; Noji et al., 1993), and Balsfjorden (125–175 mg POC m^{-3}; Wassmann et al., 2000) during winter (November–March). However, the concentration of suspended POC at KaF showed an unexpected pattern. During January and February, the concentrations were higher (55–114 mg POC m^{-3}) than in December and March (20–40 mg POC m^{-3}, except in December at 90 m: 132 mg POC m^{-3}). We hypothesize that the stronger winds in January and February caused more resuspension of organic material from the seafloor, as previously suggested for Ramfjorden (Noji et al., 1993). This speculation seems to be supported by the lower Chl a:(Chl a + Phaeo) ratios (0.23–0.31; Table S2) and the very high POC: Chl a ratios (1954–4031; Table S2) of the suspended biomass in January and February compared to December and March (Chl a:(Chl a + Phaeo) ratios of 0.37–0.44, POC: Chl a ratios of 198–1270; Table S2). The C: N ratios, however, did not change very much. Further, the NorFjords160 model results suggest that horizontal currents were strongest in January and February, particularly at the location and depth of the lowest sediment trap (90 m; **Figure 5**). We interpret this result as an additional indication for increased resuspension in this period. The downward flux of POC at KaF seemed to follow the same pattern as the suspended POC concentration, because it was slightly higher in January and February than in December and March (**Figure 8b** and **d**). Overall, the downward POC flux (**Figure 8d**) fell in a similar range as reported from Adventfjorden (Wiedmann et al., 2016), Ramfjorden (Noji et al., 1993), and Balsfjorden (Lutter et al., 1989) in December to March. Much of the sinking matter seems likely to have been previously resuspended material,

however, given the high winter C: N and POC: Chl a ratios (8.17–9.45 and 1065–2263, respectively, at 90 m during January–March). This likely contribution of resuspended material is especially important to remember when estimating how much biomass was added to the benthic system during winter.

In line with the low concentrations of Chl a and POC during winter, the zooplankton abundance declined between November and December and remained low until mid-March (< 143 ind. m^{-3} at 0–100 m; **Figure 9**). Analyses of backscatter data from the ADCPs deployed near KaF support our findings because a weak signal of diel vertical migration was found during winter (Blom, 2021). The zooplankton composition and abundance were similar to those reported from other sub-Arctic and Arctic fjords (Weslawski et al., 1991; Stübner et al., 2016; Michelsen et al., 2017; Coguiec et al., 2021; Barth-Jensen et al., 2022). The few copepods found were mainly *Pseudocalanus*, *Oithona*, and *Microcalanus* (**Figure 9**, Table S4), which supports earlier findings that small copepods use active winter survival strategies because they cannot store great amounts of lipids (Ashjian et al., 2003). For example, *Pseudocalanus* has been observed to maintain a low population throughout winter in Kongsfjorden, Svalbard, possibly by switching from herbivory to omnivory and carnivory (Lischka and Hagen, 2005). The omnivorous copepod *Oithona* (Wiborg, 1954; Kattner et al., 2003; Lischka and Hagen, 2007) has been suggested to graze and even reproduce during winter (Ashjian et al., 2003). In addition to phytoplankton (Pond and Ward, 2011; Zamora-Terol and Saiz, 2013), and protozooplankton (Nishibe et al., 2010), *Oithona* has also been observed to include zooplankton fecal pellets into their diet when other food is scarce (Gonzalez and Smetacek, 1994). Whether *Oithona* efficiently ingests fecal pellets (Gonzalez and Smetacek, 1994) or primarily fragments them (Reigstad et al., 2005) is still debated, but irrespective of the definitive process, sloppy feeding and fragmentation of pellets and aggregates by copepods likely takes place. This process can make organic carbon more accessible for degradation by bacteria (Iversen and Poulsen, 2007; Svensen et al., 2014). It may also be linked to the "microbial gardening" hypothesis (Mayor et al., 2014), which suggests that bacterial colonization turns sinking particles into attractive prey for ciliates, which may, in turn, be preyed upon by parasitic alveolates, dinoflagellates, and copepods. Though all key taxa of the microbial gardening hypothesis have been observed in high latitude fjords during winter (this study; Seuthe et al., 2011; Marquardt et al., 2016; 2019), so far we can only speculate that microbial gardening may take place in fjords during winter and contribute to effective carbon recycling in the pelagic system and a weak downward carbon flux.

We observed small numbers of the herbivorous *Calanus* (7.3–16.3 ind. m^{-3}) between January and March at KaF. In general, mainly *C. finmarchicus* and *C. glacialis* are present in fjords in northern Norway, sometimes accompanied by *C. hyperboreus* (Choquet et al., 2017) and *C. helgolandicus* (Coguiec et al., 2021). In a genetic study, Choquet et al. (2018) showed that the prosome length

of CIV, CV, and female *C. finmarchicus* and *C. glacialis* largely overlaps in the north Norwegian fjord Skjerstadfjorden (approximately 67.3° N, 15.1° E) and that speciation was best done with genetic testing. A recent study in Balsfjorden identified all four *Calanus* species by metabarcoding (Coguiec et al., 2021); however, this processing was unavailable for this study and thus we cannot reliably state which *Calanus* species were present at KaF. North Norwegian populations of *Calanus* are commonly assumed to diapause in cool waters at 700–1200 m depth off the shelf break (Halvorsen et al., 2003) and survive the winter on lipid reserves (Falk-Petersen et al., 2009) before being transported cross-shelf towards the coast during late winter/spring (Opdal and Vikebø, 2015). Based on our observation of *Calanus* at KaF, we speculate that a few *Calanus* may also survive the winter in shallow fjords such as Kaldfjorden, as previously suggested by, e.g., Skarðhamar et al. (2007) and Espinasse et al. (2016). In our results the effect of Atlantic-derived water inflow becomes apparent in both hydrographic observations and hydrodynamic model results starting in mid-March (**Figures 3** and **4**); however, interaction between water masses on the shelf and shelf break can mix species present in Atlantic Water into Norwegian Coastal Water throughout winter, and thus zooplankton at KaF may originate from both water masses.

Spring (April to May)
Surface waters at KaF warmed (2 to 6°C) and freshened (S = 33.7 to 32.6) during spring. These ranges are similar to previous reports for surface waters in April–May from other northern Norwegian fjords (e.g., warming from 2 to 6°C at outer Malangen, 1.5 to 7°C at Altafjorden, and 1 to 8°C at Balsfjorden, outer Malangen/outer Altafjorden, with surface salinities > 30.3; Mankettikkara, 2013). The wider ranges of temperature and salinity found in these fjords compared to KaF, suggests that these fjords might have been influenced by a more continental climate (colder winters/warmer spring) and by larger river run-off (causing lower surface salinities) during spring. Further, interannual variability needs to be taken into account. Nevertheless, we consider Kaldfjorden to be a typical North Norwegian fjord during spring. In early April, both the field observations and the NorFjords160 model suggested inflow of saline and, compared to local surface waters, warm water below 50 m at KaF (**Figures 3–6**). Previous investigations have shown that the troughs at the North Norwegian shelf break can facilitate cross-shelf advection of AW towards the coast (Sundby, 1984). This process seems to be further promoted by an unstratified water column (common between October and May/June), along-shelf winds, and tides (Moseidjord et al., 1999; Skarðhamar and Svendsen, 2005). If this cross-shelf water transport takes place, waters with a large fraction of AW are likely to spill over the 70–90 m deep entrance to Vengsøyfjorden (**Figure 1b**) and be advected towards Kaldfjorden. The water column stratification at KaF between April and May (**Figure 4**) was plausibly re-established by such conditions; i.e., saline AW-influenced water inflow at depth in combination with surface

freshening from snowmelt and surface warming (after early April, average daily air temperatures were greater than sea surface temperature for most of the day).

The increasing day-length during spring, the low zooplankton abundances (**Figures 9** and **10**), and the very weakly stratified water column (**Figure 3b**) presumably allowed upward mixing of nitrate from depth to surface (**Figure 7**) likely limiting grazing pressure and promoting the build-up of the autotrophic biomass at KaF prior to our sampling in early April (maximum Chl *a* concentration of 6.9–7.2 µg Chl *a* L^{-1} at 5–15 m in April; **Figure 8**). The low C: N ratios (5.7–5.9 at 5–30 m), the high Chl *a*:(Chl *a* + Phaeo) ratios (0.53–0.57 at 5–30 m), and the low POC: Chl *a* ratios (35–39 at 5–30 m) clearly suggest the presence of freshly produced biomass during an ongoing spring bloom. Thus, both the timing and the intensity of the bloom observed at KaF were typical for Northern Norway (Eilertsen et al., 1981; Lutter et al., 1989; Reigstad and Wassmann, 1996; Falkenhaug et al., 1997; Wassmann et al., 2000; Eilertsen and Degerlund, 2010). Further, our findings support previous studies, which claim that phytoplankton spring blooms in high latitudes can take place in waters without a shallow mixed layer (Townsend et al., 1992; Eilertsen, 1993), in contrast to Sverdrup's theory (1953). At KaF, an unstratified water column was present for a short period before our April field work (**Figure 2c**), which agrees with the critical turbulence hypothesis (Townsend et al., 1992; Behrenfeld and Boss, 2014). During the high Chl *a* concentration in April a strong downward flux of Chl *a* was also observed throughout the whole water column (2.9–3.1 mg Chl *a* m^{-2} d^{-1} at 20–90 m; **Figure 8a** and **c**). We presume that the high algal biomass and low zooplankton abundance (and associated low grazing pressure) allowed this downward flux of Chl *a* in early April (**Figure 9**).

The suspended POC concentrations (at 5 and 15 m) were high at KaF in April (253–264 mg POC m^{-3}), but lower than in October (232–315 mg POC m^{-3}). This pattern differs from previous findings in Adventfjorden and Balsfjorden, where annually the highest POC concentrations were found during spring (Wassmann et al., 2000; Wiedmann et al., 2016). We speculate that the POC concentrations at KaF in spring could have been lower than in other fjords, because no major rivers or glaciers terminate into Kaldfjorden, which tend to be a source of (terrestrial) POC (McMahon and Patching, 1984; Sejr and Rysgaard, 2007; Kuliński et al., 2014). Unlike the suspended POC concentrations, the downward flux of POC was in the range of previous observations (117–158 mg POC m^{-2} d^{-1} at KaF: 150–600 mg POC m^{-2} d^{-1} at 30–100 m in Malangen; Keck and Wassmann, 1996; and 235–635 mg POC m^{-2} d^{-1} in Adventfjord; Wiedmann et al., 2016). In addition, observations from KaF resembled previous findings, because the strongest downward POC flux of the year took place in late summer/autumn (**Figure 8d**; Keck and Wassmann, 1996; Wiedmann et al., 2016). Results from Adventfjorden suggested that high precipitation and run-off of lithogenic material during autumn may have caused flocculation and resulted in the high downward POC flux during autumn (Wiedmann et al., 2016). This

argument, however, seems invalid at KaF, because precipitation was negligible prior to our field sampling in October and only small rivers drain into Kaldfjorden (**Figure 2b**). As the NorFjords160 model indicated that currents at 90 m were stronger during autumn than in spring (**Figure 5**), we presume that more biomass was resuspended from the seafloor in autumn, resulting in a higher downward POC flux than during spring. In addition, the model results suggest a high spatial and seasonal variability of currents in Kaldfjorden, which may result in very local resuspension events and, in turn, explain the differences in the Chl *a* and POC flux found at three locations in Kaldfjorden (this study; Lalande et al., 2016).

Compared to winter, zooplankton abundance was high in April, when small zooplankton (< 2.5 mm) dominated the community: *Microcalanus* spp., *Oithona* spp., and meroplankton (larvae of Cirripedia and benthic Polychaeta). This predominance of small species was likely even more pronounced, as zooplankton < 2.5 mm are notably undersampled by a zooplankton net with a mesh size of 180 μm (Nichols and Thompson, 1991). The general species composition mirrors observations from Porsangerfjorden (Michelsen et al., 2017) and Adventfjorden (Stübner et al., 2016), and we presume that some taxa that were active all winter (*Oithona*, *Microcalanus*) may have started grazing on the developing phytoplankton bloom and potentially produced offspring during early spring. *Oithona* spp. have been noted as the most abundant in Atlantic water (mostly *O. similis*, but also *O. atlantica*; Weydmann et al., 2014; Gluchowska et al., 2017), and thus their abundance at KaF in April further supports the indications by the model and hydrographic observations of Atlantic-influenced water.

The most pronounced increase in zooplankton abundance took place between April and May. In this period a strong increase in ADCP backscatter strength, likely from zooplankton conducting dial vertical migration, was also observed by Blom (2021). The species composition changed considerably compared to winter. Larger species dominated in May, primarily *Calanus* and *Metridia* (likely *M. longa,* based on observations in nearby Balsfjord; Eilertsen et. al., 1981; Barthel et. al, 1995; Coguiec et al., 2021). High concentrations and dominance of the herbivorous *C. finmarchicus* have previously been reported for North Norwegian fjords during spring: Malangen (Falkenhaug et al., 1997), Balsfjorden (Tande and Slagstad, 1992), and Porsangerfjorden (Michelsen et al., 2017). A common assumption is that *C. finmarchicus* (Halvorsen et al., 2003) and *C. hyperboreus* (Hirche, 1997; Falk-Petersen et al., 2009) are advected from their overwintering location at the shelf break during late winter/spring. We suggest that advection of *Calanus* likely also happened in Kaldfjorden from March to May (**Figures 3** and **6**), because during this period, Blom (2021) found an increase in ADCP backscatter strength throughout the water column at two mooring stations 3.7 km north and 1.55 km south of KaF. As the increase in the backscatter strength is an indication of more zooplankton present, and as the increase was first found north of KaF (closer to the fjord mouth) and shortly after also south of KaF, these observations seem to suggest advection of *Calanus* from the shelf. Once in the fjord, the advected *Calanus* adults as well as the developing copepodites likely grazed on the accumulated autotrophic biomass in the upper 20 m in Kaldfjorden. This grazing likely caused the strong surface backscatter layer reported by Blom (2021), and reduced and degraded the suspended autotrophic biomass drastically (**Figure 8a**, Table S2). In turn, as less autotrophic biomass was present in the water column, less material was available to sink and thus the downward Chl *a* and POC flux declined in May compared to April (**Figure 7c**, Table S3). From April onwards, the surface nutrient concentrations were nearly depleted in the surface waters of Kaldfjorden (**Figures 7**, S3, and S4) and the re-established stratification (**Figure 3c**) likely hindered vertical mixing and upward flux of nutrients from the bottom layer in the fjord, where the concentrations were still high. We thus propose that the decline after the phytoplankton spring bloom was caused not only by the high number of zooplankton but also by limited nutrient concentrations in the euphotic zone.

Spatial context —Is KaF representative of the whole fjord?

Station KaF is located approximately midway in Kaldfjorden on the eastern slope of the fjord (**Figure 1b**). The hydrodynamic model results indicate a rather complex circulation (**Figure 5**); however, even with seasonal variations, velocities are low. Especially at depth, the outer and central parts of the fjord remain connected through the along-slope flow, while the innermost, shallower part of the fjord is more decoupled. KaF is situated on the rim of an eddy-like feature in the central part of the fjord and, due to its position on sloping topography, is influenced by the along-slope flow in the main fjord basin (**Figure 5**). Observations from concurrent long-term moorings deployed approximately 3.7 km north and 1.55 km south of KaF indicate very similar seasonal patterns in particle load and flux at both locations (Lalande et al., 2020; Blom, 2021). The main differences between those moorings were a higher flux during winter and earlier onset of elevated particle load in spring at the northern mooring compared to the mooring south of KaF, suggesting that the timing of processes at KaF is representative for average conditions in the central and outer Kaldfjorden. Hydrographic observations and water samples from three repeated east–west transects at different latitudes in Kaldfjorden (figure 1 in Jones et al., 2020) show fairly uniform distribution of temperature, salinity and density across the fjord (Jones et al., 2020; Renner, 2020b), which is expected for a narrow fjord without major freshwater sources like large rivers or glaciers. Comparison of water properties at the three transects, as reported by Jones et al. (2020), supports the results from the long-term moorings (Lalande et al., 2020; Blom, 2021) that physical, chemical and biological parameters and their variability are similar throughout the fjord, but with slight offsets in timing and a stronger influence of shelf waters in the outer part versus land influence (colder temperatures and more freshwater) in the inner part of Kaldfjorden. We therefore are confident

that our observations at KaF are representative for the average state of the fjord with the caveat that the inner fjord might be less well represented by our findings.

Conclusion and implications

Studies during recent years have shown that biological activity in fjords is not totally at rest during winter (Darnis et al., 2012; Berge et al., 2015b), and year-round field studies have improved the overall understanding of fjord ecosystems (Seuthe et al., 2011; Juul-Pedersen et al., 2015; Sørensen et al., 2015; Marquardt et al., 2016; Wiedmann et al., 2016; Michelsen et al., 2017). Ecological processes during winter, however, are still little studied and poorly understood, even though winter has been identified as an important season for "resetting" the fjord ecosystem by, for example, upwelling of nutrients (in Kaldfjorden; Jones et al., 2020). Our findings show that Kaldfjorden is a typical sub-Arctic fjord with regard to hydrography, zooplankton composition and abundance, and Chl *a* and POC concentrations and downward fluxes in the transition from autumn to winter and spring. Therefore, we see Kaldfjorden as a representative fjord and presume that processes observed here are likely also occurring in other ice-free high latitude fjords.

The major finding in this study was the tight coupling between hydrography, the suspended Chl *a* and POC concentrations, and the downward flux of these parameters. The NorFjords160 hydrodynamic model results support previous assumptions that strong currents occur in fjords during winter and may lead to biomass resuspension from the seafloor in an unstratified water column (Noji et al., 1993; Wiedmann et al., 2016). Careful interpretation of the downward flux of organic matter during winter is therefore needed, because only (small) parts of the downward flux represent additional nutritional input to the benthic ecosystem. In addition, a comparison of our findings with the observations from two long-term sediment traps in Kaldfjorden (Lalande et al., 2020) illustrates that these resuspension effects may be very local, potentially tied to topography, and result in dissimilar Chl *a* and POC downward fluxes in different parts of Kaldfjorden. Therefore, we suggest that the common understanding of estuarine circulation (Mann and Lazier, 2006) is only a very rough approximation of the actual circulation in many fjords and underestimates the spatial and temporal variability of processes with biological relevance, such as biomass resuspension. Based on our field observations, we speculate that the resuspended biomass may provide food for the heterotrophic winter community of nano- to mesoplankton, including nauplii, in the fjord. This provision may happen through either resuspended phytoplankton resting stages (Berkman et al., 1986) or "microbial gardening" (Mayor et al., 2014). The combination of hydrographic and biological field observations and hydrodynamic model results allowed us to further support previous speculations and simulations of cross-shelf zooplankton advection during early spring (Halvorsen et al., 2003; Opdal and Vikebø, 2015). We point out that this study covers only one winter season, and physical and chemical conditions as well as biological processes such as interactions between species may vary considerably from year to year.

Our study provides further evidence for biological activity in high latitude fjords during winter. An increasing number of fjords, including Kaldfjorden, are used by the aquaculture industry, and winter observations are crucial for securing improved knowledge on the year-round conditions. In 2016, 1175 active aquaculture licenses for salmon and rainbow trout were registered along the Norwegian coast (Statistics Norway, www.ssb.no), and numbers have been increasing since then (1264 licenses in 2019). Though sedimentation of organic matter seemed not to change in direct proximity to a producing fish farm, the isotope signal of organic remnants from the farm was found at least 900 m from the farm in Uggdalsfjorden, Western Norway (Kutti et al., 2007). In a shallower fjord like Kaldfjorden with a complex circulation pattern, remnants may be spread even more, and the same could apply to pesticides used against the salmon louse, which can also affect non-target copepods (Escobar-Lux et al., 2019). Though the use of these pesticides has generally declined during the last years (Grefsrud et al., 2019), little is known about how eggs and nauplii react to these pesticides (Escobar-Lux et al., 2019) or how they affect small copepods. Evaluating the effect of aquaculture industry on the pelagic fjord ecosystem during winter is hardly possible, but we suspect that smaller copepods have even lower tolerance for pesticides than large ones. Therefore, we strongly recommend that the increasing knowledge about fjord winter ecology, as provided by this study, be included in future fjord management decisions to improve the environmentally sustainable use of these important coastal ecosystems.

Data accessibility statement

The CTD data used in this study are accessible at:

Renner, A. 2020a. Hydrography at 69.746° N, 18.683° E (Kaldfjorden, Troms, Norway), Oct 2017–May 2018. Norwegian Marine Data Centre, https://doi.org/10.21335/NMDC-625749953.

The nutrient data in this study are publicly available at: doi:10.21335/NMDC-646962623.

The biological data from this study are available at:

Walker, EZ, Wiedmann, I. 2022. Seasonality of suspended and exported Chl *a* and POC and Zooplankton at station KaF, Kaldfjorden (WHALE project). https://doi.org/10.21335/NMDC-2116003163.

Supplemental files

The supplemental files for this article can be found as follows:

Figures S1–S4. Tables S1–S4.Docx.

Funding

Competing interests

The authors declare no competing interests.

Author contributions

Conceptual idea of the work: AR, IW, ZW. Acquisition and analyses of field data: ZW, AR, IW, EJ.

Numerical modelling: AN, JS.

Data interpretation and contribution to writing the manuscript: ZW, IW, AR, AN, JS, EJ.

Approved the submitted version for publication: ZW, IW, AR, AN, JS, EJ.

References

Albretsen, J, **Sperrevik, AK**, **Staalstrøm, A**, **Sandvik, AD**, **Vikebø, F**, **Asplin, L**. 2011. NorKyst-800 report No.1 user manual and technical descriptions, in *Fisken og Havet*. Institute of Marine Research. Available at https://www.hi.no/resources/publikasjoner/fisken-og-havet/2011/fh_2-2011_til_web.pdf. Accessed 19 May 2021.

Arctic Monitoring and Assessment Programme. 2018. *AMAP assessment 2018: Arctic Ocean acidification.* Tromsø, Norway: Arctic Monitoring and Assessment Programme. 187 p.

Ashjian, CJ, **Campbell, RG**, **Welch, HE**, **Butler, M**, **Van Keuren, D**. 2003. Annual cycle in abundance, distribution, and size in relation to hydrography of important copepod species in the western Arctic Ocean. *Deep-Sea Research Part I* **50**(10): 1235–1261. DOI: https://dx.doi.org/10.1016/S0967-0637(03)00129-8.

Asplin, L, **Albretsen J**, **Johnsen, IA**, **Sandvik, AD**. 2020. The hydrodynamic foundation for salmon lice dispersion modeling along the Norwegian coast. *Ocean Dynamics* **70**(8): 1151–1167. DOI: https://dx.doi.org/10.1007/s10236-020-01378-0.

Barth, JAC, **Veizer, J**, **Mayer, B**. 1998. Origin of particulate organic carbon in the upper St. Lawrence: isotopic constraints. *Earth and Planetary Science Letters*, **162**(1–4): 111–121, DOI: https://dx.doi.org/10.1016/S0012-821X(98)00160-5.

Barth-Jensen, C, **Daase, M**, **Ormańczyk, MR**, **Varpe, Ø**, **Kwaśniewski, S**, **Svensen, C**. 2022. High abundances of small copepods early developmental stages and nauplii strengthen the perception of a non-dormant Arctic winter. *Polar Biology* **45**: 675–690. DOI: https://doi.org/10.1007/s00300-022-03025-4.

Barthel, KG, **Noji, TT**, **Noji, CIM**. 1995. Zooplankton dynamics during the onset of winter in a northern Norwegian fjord. Vertical distribution and metabolic activity in relation to phytoplankton and sedimentation. *Sarsia* **80**(1): 23–32. DOI: https://dx.doi.org/10.1080/00364827.1995.10413575.

Behrenfeld, MJ, **Boss, ES**. 2014. Resurrecting the ecological underpinnings of ocean plankton blooms. *Annual Review of Marine Science* **6**(1): 167–194. DOI: https://dx.doi.org/10.1146/annurev-marine-052913-021325.

Berge, J, **Daase, M**, **Renaud, PE**, **Ambrose, WG**, Jr., **Darnis, G**, **Last, KS**, **Leu, E**, **Cohen, JH**, **Johnsen, G**, **Moline, MA**, **Cottier, F**, **Varpe, Ø**, **Shunatova, N**, **Bałazy, P**, **Morata, N**, **Massabuau, JC**, Falk-**Petersen, S**, **Kosobokova, K**, **Hoppe, CJM**, **Węsławski, JM**, **Kuklinski, P**, **Legeżynska, J**, **Nikishina, D**, **Cusa, M**, **Kędra, M**, **Włodarska-Kowalczuk, M**, **Vogedes, D**, **Camus, L**, **Tran, D**, **Michaud, E**, **Gabrielsen, TM**, **Granovitch, A**, **Gonchar, A**, **Krapp, R**, **Callesen, TA**. 2015a. Unexpected levels of biological activity during the polar night offer new perspectives on a warming Arctic. *Current Biology* **25**(19): 2555–2561. DOI: https://dx.doi.org/10.1016/j.cub.2015.08.024.

Berge, J, **Renaud, PE**, **Darnis, G**, **Cottier, F**, **Last, K**, **Gabrielsen, TM**, **Johnsen, G**, **Seuthe, L**, **Węsławski, JM**, **Leu E**, **Moline, M**, **Nahrgang, J**, **Søreide, JE**, **Varpe, Ø**, **Lønne, OJ**, **Daase, M**, **Falk-Petersen, S**. 2015b. In the dark: A review of ecosystem processes during the Arctic polar night. *Progress in Oceanography* **139**: 258–271. DOI: https://dx.doi.org/10.1016/j.pocean.2015.08.005.

Berkman, PA, **Marks, DS**, **Shreve, GP**. 1986. Winter sediment resuspension in McMurdo Sound, Antarctica, and its ecological implications. *Polar Biology* **6**(1): 1–3. DOI: https://dx.doi.org/10.1007/BF00446234.

Blom, M. 2021. Drivers of seasonal and diurnal particulate material load patterns in northern Norwegian fjords [Master thesis]. Akureyri, Iceland: University Centre of the Westfjords, University of Akureyri. 91 p.

Boyd, PW, **Claustre, H**, **Levy, M**, **Siegel, DA**, **Weber T**. 2019. Multi-faceted particle pumps drive carbon sequestration in the ocean. *Nature* **568**: 327–335. DOI: https://dx.doi.org/10.1038/s41586-019-1098-2.

Carvajalino-Fernández, MA, **Sævik, PN**, **Johnsen, IA**, **Albretsen, J**, **Keeley, NB**. 2020. Simulating particle organic matter dispersal beneath Atlantic salmon fish farms using different resuspension approaches. *Marine Pollution Bulletin* **161**: 111685. DOI: https://dx.doi.org/10.1016/j.marpolbul.2020.111685.

Choquet, M, **Hatlebakk, M**, **Dhanasiri, AKS**, **Kosobokova, K**, **Smolina, I**, **Søreide, JE**, **Svensen, C**, **Melle, W**, **Kwaśniewski, S**, **Eiane, K**, **Daase, M**, **Tverberg, V**, **Skreslet, S**, **Bucklin, A**, **Hoarau, G**.

2017. Genetics redraws pelagic biogeography of *Calanus*. *Biology Letters* **13**(12): 20170588. DOI: https://dx.doi.org/10.1098/rsbl.2017.0588.

Choquet, M, Kosobokova, K, Kwaśniewski, S, Hatlebakk, M, Dhanasiri, AKS, Melle, W, Daase, M, Svensen, C, Søreide, JE, Hoarau, G. 2018. Can morphology reliably distinguish between the copepods *Calanus finmarchicus* and *C. glacialis*, or is DNA the only way? *Limnology and Oceanography: Methods* **16**(4): 237–252. DOI: https://dx.doi.org/10.1002/lom3.10240.

Cloern, JE, Foster, SQ, Kleckner, AE. 2014. Phytoplankton primary production in the world's estuarine-coastal ecosystems. *Biogeosciences* **11**(9): 2477–2501. DOI: https://dx.doi.org/10.5194/bg-11-2477-2014.

Coguiec, E, Ershova, EA, Daase, M, Vonnahme, TR, Wangensteen, OS, Gradinger, R, Præbel, K, Berge, J. 2021. Seasonal variability in the zooplankton community structure in a sub-Arctic fjord as revealed by morphological and molecular approaches. *Frontiers in Marine Science* **8**: 705042. DOI: https://dx.doi.org/10.3389/fmars.2021.705042.

Coppola, L, Roy-Barman, M, Wassmann, P, Mulsow, S, Jeandel, C. 2002. Calibration of sediment traps and particulate organic carbon export using 234Th in the Barents Sea. *Marine Chemistry* **80**(1): 11–26. DOI: https://dx.doi.org/10.1016/S0304-4203(02)00071-3.

Daase, M, Eiane, K. 2007. Mesozooplankton distribution in northern Svalbard waters in relation to hydrography. *Polar Biology* **30**(8): 969–981. DOI: https://dx.doi.org/10.1007/s00300-007-0255-5.

Dalsøren, SB, Albretsen, J, Asplin, L. 2020. New validation method for hydrodynamic fjord models applied in the Hardangerfjord, Norway. *Estuarine Coastal and Shelf Science* **246**: 107028. DOI: https://dx.doi.org/10.1016/j.ecss.2020.107028.

Darnis, G, Robert, D, Pomerleau, C, Link, H, Archambault, P, Nelson, RJ, Geoffroy, M, Tremblay, JÉ, Lovejoy, C, Ferguson, SH, Hunt, BPV, Fortier, L. 2012. Current state and trends in Canadian Arctic marine ecosystems: II. Heterotrophic food web, pelagic-benthic coupling, and biodiversity. *Climate Change* **115**(1): 179–205. DOI: https://dx.doi.org/10.1007/s10584-012-0483-8.

Egbert, GD, Erofeeva, SY. 2002. Efficient inverse modeling of barotropic ocean tides. *Journal of Atmospheric and Oceanic Technology* **19**(2): 183–204. DOI: https://dx.doi.org/10.1175/1520-0426(2002)019<0183:EIMOBO>2.0.CO;2.

Eilertsen, HC. 1993. Spring blooms and stratification. *Nature* **363**(6424): 24.

Eilertsen, HC, Degerlund, M. 2010. Phytoplankton and light during the northern high-latitude winter. *Journal of Plankton Research* **32**(6): 899–912. DOI: https://dx.doi.org/10.1093/plankt/fbq017.

Eilertsen, HC, Frantzen, S. 2007. Phytoplankton from two sub-Arctic fjords in Northern Norway 2002-2004: I. Seasonal variations in chlorophyll *a* and bloom dynamics. *Marine Biology Research* **3**(5): 319–332. DOI: https://dx.doi.org/10.1080/17451000701632877.

Eilertsen, HC, Schei, B, Taasen, JP. 1981. Investigations on the plankton community of Balsfjorden, Northern Norway. *Sarsia* **66**(2): 129–141. DOI: https://dx.doi.org/10.1080/00364827.1981.10414530.

Eilertsen, HC, Taasen, JP. 1984. Investigations on the plankton community of Balsfjorden, Northern Norway. The phytoplankton 1976–1978. Environmental factors, dynamics of growth, and primary production. *Sarsia* **69**(1): 1–15. DOI: https://dx.doi.org/10.1080/00364827.1984.10420584.

Engel, A, Goldthwait, S, Passow, U, Alldredge, A. 2002. Temporal decoupling of carbon and nitrogen dynamics in a mesocosm diatom bloom. *Limnology and Oceanography* **47**(3): 753–761. DOI: https://dx.doi.org/10.4319/lo.2002.47.3.0753.

Escobar-Lux, RH, Fields, DM, Browman, HI, Shema, SD, Bjelland, RM, Agnalt, AL, Skiftesvik, AB, Samuelsen, OB, Durif, CMF. 2019. The effects of hydrogen peroxide on mortality, escape response, and oxygen consumption of *Calanus* spp. *FACETS* **4**: 626–637. DOI: https://dx.doi.org/10.1139/facets-2019-0011.

Espinasse, B, Basedow, SL, Tverberg, V, Hattermann, T, Eiane, K. 2016. A major Calanus finmarchicus overwintering population inside a deep fjord in northern Norway: Implications for cod larvae recruitment success. *Journal of Plankton Research* **38**(3): 604–609. DOI: https://dx.doi.org/10.1093/plankt/fbw024.

Falkenhaug, T, Tande, K, Timonin, A. 1997. Spatio-temporal patterns in the copepod community in Malangen, Northern Norway. *Journal of Plankton Research* **19**(4): 449–468. DOI: https://dx.doi.org/10.1093/plankt/19.4.449.

Falk-Petersen, IB. 1982. Ecological investigations on the zooplankton community of Balsfjorden, Northern Norway. *Sarsia* **67**(1): 69–78. DOI: https://dx.doi.org/10.1080/00364827.1982.10421335.

Falk-Petersen, S, Mayzaud, P, Kattner, G, Sargent, JR. 2009. Lipids and life strategy of Arctic *Calanus*. *Marine Biology Research* **5**(1): 18–39. DOI: https://dx.doi.org/10.1080/17451000802512267.

Friedland, KD, Record, NR, Asch, RG, Kristiansen, T, Saba, VS, Drinkwater, KF, Henson, S, Leaf, RT, Morse, RE, Johns, DG, Large, SI, Hjøllo, SS, Nye, JA, Alexander, MA, Ji, R. 2016. Seasonal phytoplankton blooms in the North Atlantic linked to the overwintering strategies of copepods. *Elementa Science of the Anthropocene* **4**: 000099. DOI: https://dx.doi.org/10.12952/journal.elementa.000099.

Gluchowska, M, Dalpadado, P, Beszczynska-Möller, A, Olszewska, A, Ingvaldsen, RB, Kwasniewski, S. 2017. Interannual zooplankton variability in the main pathways of the Atlantic water flow into the Arctic Ocean (Fram Strait and Barents Sea branches). *ICES Journal of Marine Science* **74**(7): 1921–1936. DOI: https://dx.doi.org/10.1093/icesjms/fsx033.

Gonzalez, HE, Smetacek, V. 1994. The possible role of the cyclopoid copepod *Oithona* in retarding vertical flux of zooplankton faecal material. *Marine Ecology Program Series* **113**: 233–246.

Grefsrud, ES, Svåsand, T, Glover, K, Husa, V, Hansen, PK, Samuelsen, OB, Sandlund, N, Stien, LH. 2019. *Risikorapport norsk fiskeoppdrett—Miljøeffekter av lakseoppdrett.* Havforskningsinstituttet. Available at https://www.hi.no/hi/nettrapporter/fisken-og-havet-2019-5#sec-miljoeffekter-pa-non-target-arter-ved-bruk-av-legemidler. Accessed 20 July 2020.

Haidvogel, DB, Arango, H, Budgell, WP, Cornuelle, BD, Curchitser, E, Di Lorenzo, E, Fennel, K, Geyer, WR, Hermann, AJ, Lanerolle, L, Levin, J, McWilliams, JC, Miller, AJ, Moore, AM, Powell, TM, Shchepetkin, AF, Sherwood, CR, Signell, RP, Warner, JC, Wilkin, J. 2008. Ocean forecasting in terrain-following coordinates: Formulation and skill assessment of the regional ocean modeling system. *Journal of Computational Physics* **227**(7): 3595–3624. DOI: https://dx.doi.org/10.1016/j.jcp.2007.06.016.

Halvorsen, E, Tande, KS, Edvardsen, A, Slagstad, D, Pedersen, OP. 2003. Habitat selection of overwintering *Calanus finmarchicus* in the NE Norwegian Sea and shelf waters off Northern Norway in 2000-02. *Fisheries and Oceanography* **12**(4–5): 339–351. DOI: https://dx.doi.org/10.1046/j.1365-2419.2003.00255.x.

Hegseth, EN, Svendsen, H, von Quillfeldt, CH. 1995. Phytoplankton in fjords and coastal waters of Northern Norway: Environmental conditions and dynamics of the spring bloom, in Skjoldal, HR, Hopkins, C, Erikstad, KE, Leinaas, HP eds., *Ecology of fjords and coastal waters. Proceedings of the Mare Nor Symposium on the Ecology of Fjords and Coastal Waters.* Amsterdam, the Netherlands: Elsevier: 5–72.

Helland-Hansen, B, Nansen, F. 1909. *The Norwegian Sea: Its physical oceanography based upon the Norwegian researches 1900-1904.* Kristiania, Norway: Det Mallingske bogtrykkeri. Report on Norwegian Fishery and Marine Investigation; Vol. **2**.

Hirche, HJ. 1997. Life cycle of the copepod Calanus hyperboreus in the Greenland Sea. *Marine Biology* **128**(4): 607–618. DOI: https://dx.doi.org/10.1007/s002270050127.

Holm-Hansen, O, Riemann, B. 1978. Chlorophyll *a* determination: Improvements in methodology. *Oikos* **30**(3): 438–447. DOI: https://dx.doi.org/10.2307/3543338.

Hop, H, Pearson, T, Hegseth, EN, Kovacs, KM, Wiencke, C, Kwasniewski, S, Eiane, K, Mehlum, F, Gulliksen, B, Włodarska-Kowalczuk, M, Lydersen, C, Weslawski, JM, Cochrane, S, Gabrielsen, GW, Leakey, RJG, Lønne, OJ, Zajączkowski, M, Falk-Petersen, S, Kendall, M, Wängberg, SA, Bischof, K, Voronkov, AY, Kovaltchouk, NA, Wiktor, J, Poltermann, M, di Prisco, G, Papucci, C, Gerland, S. 2002. The marine ecosystem of Kongsfjorden, Svalbard. *Polar Research* **21**(1): 167–208. DOI: https://dx.doi.org/10.3402/polar.v21i1.6480.

Iversen, MH, Poulsen, LK. 2007. Coprorhexy, coprophagy, and coprochaly in the copepods *Calanus helgolandicus*, *Pseudocalanus elongatus*, and *Oithona similis*. *Marine Ecology Program Series* **350**: 79–89. DOI: https://dx.doi.org/10.3354/meps07095.

Jones, EM, Renner, AHH, Chierici, M, Wiedmann, I, Lødemel, HH, Biuw, M. 2020. Seasonal dynamics of carbonate chemistry, nutrients and CO_2 uptake in a sub-Arctic fjord. *Elementa: Science of the Anthropocene* **8**(1): 41. DOI: https://dx.doi.org/10.1525/elementa.438.

Juul-Pedersen, T, Arendt, KE, Mortensen, J, Blicher, ME, Søgaard, DH, Rysgaard, S. 2015. Seasonal and interannual phytoplankton production in a sub-Arctic tidewater outlet glacier fjord, SW Greenland. *Marine Ecology Program Series* **524**: 27–38. DOI: https://dx.doi.org/10.3354/meps11174.

Kattner, G, Albers, C, Graeve, M, Schnack-Schiel, SB. 2003. Fatty acid and alcohol composition of the small polar copepods, *Oithona* and *Oncaea*: Indication on feeding modes. *Polar Biology* **26**(10): 666–671. DOI: https://dx.doi.org/10.1007/s00300-003-0540-x.

Keck, A, Wassmann, P. 1996. Temporal and spatial patterns of sedimentation in the subarctic fjord Malangen, Northern Norway. *Sarsia* **80**(4): 259–276. DOI: https://dx.doi.org/10.1080/00364827.1996.10413600.

Kirby, RR, Beaugrand, G, Lindley, JA. 2008. Climate-induced effects on the meroplankton and the benthic-pelagic ecology of the North Sea. *Limnology and Oceanography* **53**(5): 1805–1815. DOI: https://dx.doi.org/10.4319/lo.2008.53.5.1805.

Kuliński, K, Kędra, M, Legeżyńska, J, Gluchowska, M, Zaborska, A. 2014. Particulate organic matter sinks and sources in high Arctic fjord. *Journal of Marine Systems* **139**: 27–37. DOI: https://dx.doi.org/10.1016/j.jmarsys.2014.04.018.

Kutti, T, Ervik, A, Hansen, PK. 2007. Effects of organic effluents from a salmon farm on a fjord system. I. Vertical export and dispersal processes. *Aquaculture* **262**(2): 367–381. DOI: https://dx.doi.org/10.1016/j.aquaculture.2006.10.010.

Lalande, C, Dunlop, K, Renaud, PE, Nadaï, G, Sweetman, AK. 2020. Seasonal variations in downward particle fluxes in Norwegian fjords. *Estuarine Coastal and Shelf Science* **241**: 106811. DOI: https://dx.doi.org/10.1016/j.ecss.2020.106811.

Lalande, C, Moriceau, B, Leynaert, A, Morata, N. 2016. Spatial and temporal variability in export fluxes of biogenic matter in Kongsfjorden. *Polar Biology* **39**(10): 1725–1738. DOI: https://dx.doi.org/10.1007/s00300-016-1903-4.

Leu, E, Søreide, JE, Hessen, DO, Falk-Petersen, S, Berge, J. 2011. Consequences of changing sea ice cover for primary and secondary producers in the European Arctic shelf seas: Timing, quantity, and quality.

Progress in Oceanography **90**(1–4): 18–32. DOI: https://dx.doi.org/10.1016/j.pocean.2011.02.004.

Lischka, S, **Hagen, W**. 2005. Life histories of the copepods *Pseudocalanus minutus, P.* acuspes (Calanoida) and *Oithona similis* (Cyclopoida) in the Arctic Kongsfjorden (Svalbard). *Polar Biology* **28**(12): 910–921. DOI: https://dx.doi.org/10.1007/s00300-005-0017-1.

Lischka, S, **Hagen, W**. 2007. Seasonal lipid dynamics of the copepods *Pseudocalanus minutus* (Calanoida) and *Oithona similis* (Cyclopoida) in the Arctic Kongsfjorden (Svalbard). *Marine Biology* **150**(3): 443–454. DOI: https://dx.doi.org/10.1007/s00227-006-0359-4.

Lutter, S, **Taasen, JP**, **Hopkins, CCE**, **Smetacek, V**. 1989. Phytoplankton dynamics and sedimentation processes during spring and summer in Balsfjord, Northern Norway. *Polar Biology* **10**(2): 113–124. DOI: https://dx.doi.org/10.1007/BF00239156.

Mankettikkara, R. 2013. *Hydrophysical characteristics of the Northern Norwegian Coast and fjords* [dissertation]. Tromsø, Norway: UiT Norges Arktiske Universitet. Dept. of Arctic and Marine Biology. Available at https://munin.uit.no/handle/10037/5426. Accessed 20 August 2020.

Mann, KH, **Lazier, JRN**. 2006. *Dynamics of Marine ecosystems: Biological-physical interactions in the oceans*. 3rd ed. Dartmouth, Canada: Blackwell Publishing Ltd.

Marquardt, M, **Skogseth, R**, **Wiedmann, I**, **Vader, A**, **Reigstad, M**, **Cottier, F**, **Gabrielsen, TM**. 2019. Vertical export of marine pelagic protists in an ice-free high-Arctic fjord (Adventfjorden, West Spitsbergen) throughout 2011–2012. *Aquatic Microbial Ecology* **83**(1): 65–82. DOI: https://dx.doi.org/10.3354/ame01904.

Marquardt, M, **Vader, A**, **Stübner, EI**, **Reigstad, M**, **Gabrielsen, TM**. 2016. Strong seasonality of marine microbial eukaryotes in a high-Arctic fjord (Isfjorden, in West Spitsbergen, Norway). *Applied Environmental Microbiology* **82**(6): 1868–1880. DOI: https://dx.doi.org/10.1128/AEM.03208-15.

Mayor, DJ, **Sanders, R**, **Giering, SLC**, **Anderson, TR**. 2014. Microbial gardening in the ocean's twilight zone: Detritivorous metazoans benefit from fragmenting, rather than ingesting, sinking detritus. *BioEssays* **36**(12): 1132–1137. DOI: https://dx.doi.org/10.1002/bies.201400100.

McMahon, TG, **Patching, JW**. 1984. Fluxes of organic carbon in a fjord on the west coast of Ireland. *Estuarine Coastal and Shelf Science* **19**(2): 205–215. DOI: https://dx.doi.org/10.1016/0272-7714(84)90065-9.

Meire, L, **Mortensen, J**, **Rysgaard, S**, **Bendtsen, J**, **Boone, W**, **Meire, P**, **Meysman, FJR**. 2016. Spring bloom dynamics in a subarctic fjord influenced by tidewater outlet glaciers (Godthåbsfjord, SW Greenland). *Journal of Geophysical Resources: Biogeosciences* **121**(6): 1581–1592. DOI: https://dx.doi.org/10.1002/2015JG003240.

Meyers, PA. 1994. Preservation of elemental and isotopic source identification of sedimentary organic matter. *Chemical Geology* **114**(3): 289–302. DOI: https://dx.doi.org/10.1016/0009-2541(94)90059-0.

Michelsen, HK, **Svensen, C**, **Reigstad, M**, **Nilssen, EM**, **Pedersen, T**. 2017. Seasonal dynamics of meroplankton in a high-latitude fjord. *Journal of Marine Systems* **168**: 17–30. DOI: https://dx.doi.org/10.1016/j.jmarsys.2016.12.001.

Moseidjord, H, **Svenden, H**, **Slagstad, D**, **Båmstedt, U**. 1999. Sensitivity studies of circulation and ocean-shelf exchange off Northern Norway. *Sarsia* **84**(3–4): 191–198. DOI: https://dx.doi.org/10.1080/00364827.1999.10420425.

Müller, M, **Homleid, M**, **Ivarsson, K-I**, **Køltzow, MAØ**, **Lindskog, M**, **Midtbø, KH**, **Andrae, U**, **Aspelien, T**, **Berggren, L**, **Bjørge, D**, **Dahlgren, P**, **Kristiansen, J**, **Randriamampianina, R**, **Ridal, M**, **Vignes, O**. 2017. AROME-MetCoOp: A Nordic convective-scale operational weather prediction model. *Weather and Forecasting* **32**(2): 609–627. DOI: https://dx.doi.org/10.1175/WAF-D-16-0099.1.

Myksvoll, MS, **Sandvik, AD**, **Johnsen, IA**, **Skarðhamar, J**, **Albretsen, J**. 2020. Impact of variable physical conditions and future increased aquaculture production on lice infestation pressure and its sustainability in Norway. *Aquaculture Environment Interactions* **12**: 193–204. DOI: https://dx.doi.org/10.3354/aei00359.

Nichols, JH, **Thompson, AB**. 1991. Mesh selection of copepodite and nauplius stages of four calanoid copepod species. *Journal of Plankton Research* **13**(3): 661–671. DOI: https://dx.doi.org/10.1093/plankt/13.3.661.

Nishibe, Y, **Kobari, T**, **Ota, T**. 2010. Feeding by the cyclopoid copepod Oithona similis on the microplankton assemblage in the Oyashio region during spring. *Plankton and Benthos Research* **5**(2): 74–78. DOI: https://dx.doi.org/10.3800/pbr.5.74.

Noji, T, **Noji, C**, **Barthel, K**. 1993. Pelagic-benthic coupling during the onset of winter in a Northern Norwegian fjord—Carbon flow and fate of suspended particulate matter. *Marine Ecology Program Series* **93**(1–2): 89–99. DOI: https://dx.doi.org/10.3354/meps093089.

Norrbin, MF. 1996. Timing of diapause in relation to the onset of winter in the high-latitude copepods *Pseudocalanus acuspes* and *Acartia longiremis*. *Marine Ecology Program Series* **142**: 99–109. DOI: https://dx.doi.org/10.3354/meps142099.

Norrbin, MF, **Olsen, RE**, **Tande, KS**. 1990. Seasonal variation in lipid class and fatty acid composition of two small copepods in Balsfjorden, Northern Norway. *Marine Biology* **105**(2): 205–211. DOI: https://dx.doi.org/10.1007/BF01344288.

Norwegian Directorate of Fisheries. 2021. Atlantic Salmon and Rainbow Trout. Available at https://www.fiskeridir.no/English/Aquaculture/Statistics/Atlantic-salmon-and-rainbow-trout. Accessed 28 July 2021.

Norwegian Mapping Authority. 2022. At sea electronic charts (ENC). Available at https://www.kartverket.no/til-sjos/kart/elektroniske-sjokart-enc. Accessed 6 June 2021.

Norwegian Meteorological Institute. 2018. Observations and weather statistics. Available at https://seklima.met.no. Accessed 13 September 2018.

Norwegian Meteorological Institute. 2019. Dataset catalogue. Available at https://thredds.met.no. Accessed 6 May 2019.

NVE Atlas. 2021. The Norwegian Water Resources and Energy Directorate (NVE). Available at https://atlas.nve.no. Accessed 21 July 2021.

Opdal, AF, **Vikebø, FB**. 2015. Long-term stability in modelled zooplankton influx could uphold major fish spawning grounds on the Norwegian continental shelf. *Canadian Journal of Fisheries and Aquatic Sciences* **73**(2): 189–196. DOI: https://dx.doi.org/10.1139/cjfas-2014-0524.

Persson, E. 2018. A comparison between short-term sediment traps with filtered sea water and without during two contrasting periods with respect to Chl a and phytoplankton composition [Bachelor thesis]. Tromsø, Norway: UiT The Arctic University of Norway, Department of Arctic and Marine Biology. Available at: DOI: https://dx.doi.org/10.5281/zenodo.5951662. Accessed 6 February 2022.

Pond, DW, Ward, P. 2011. Importance of diatoms for Oithona in Antarctic waters. *Journal of Plankton Research* **33**(1): 105–118. DOI: https://dx.doi.org/10.1093/plankt/fbq089.

Priou, P. 2015. Associations between herbivorous zooplankton, phytoplankton and hydrography in Porsangerfjord, northern Norway [M.Sc. thesis]. Tromsø, Norway: UiT Norges arktiske universitet. Available at https://munin.uit.no/handle/10037/8270. Accessed 20 August 2020.

Reigstad, M, Riser, CW, Svensen, C. 2005. Fate of copepod faecal pellets and the role of *Oithona* spp. *Marine Ecology Program Series* **304**: 265–270. DOI: https://dx.doi.org/10.3354/meps304265.

Reigstad, M, Wassmann, P. 1996. Importance of advection for pelagic-benthic coupling in north Norwegian fjords. *Sarsia* **80**(4): 245–257. DOI: https://dx.doi.org/10.1080/00364827.1996.10413599.

Renner, AHH. 2020a. Hydrography at 69.746 N, 18.683 E (Kaldfjorden, Troms, Norway), Oct 2017–May 2018 [dataset]. Norwegian Marine Data Centre. DOI: https://dx.doi.org/10.21335/NMDC-625749953.

Renner, A. 2020b. Hydrography in Kaldfjorden, Troms, Norway, Sep 2016–Sep 2018 [dataset]. Norwegian Marine Data Centre. DOI: https://dx.doi.org/10.21335/NMDC-1539462099.

Ross, AH, Gurney, WSC, Health, MR, Hay, SJ, Henderson, EW. 1993. A strategic simulation model of a fjord ecosystem. *Limnology and Oceanography* **38**(1): 128–153. DOI: https://dx.doi.org/10.4319/lo.1993.38.1.0128.

Sejr, M, Rysgaard, S. 2007. Vertical flux of particulate organic matter in a High Arctic fjord: Relative importance of terrestrial and marine sources. Carbon cycling in Arctic marine ecosystems: Case study Young Sound. *Meddelelser Om Grønland Bioscience* **58**: 110–119.

Seuthe, L, Iversen, K, Narcy, F. 2011. Microbial processes in a high-latitude fjord (Kongsfjorden, Svalbard): II. Ciliates and dinoflagellates. *Polar Biology* **34**: 751–766. DOI: https://dx.doi.org/10.1007/s00300-010-0930-9.

Shchepetkin, AF, McWilliams, JC. 2005. The regional oceanic modeling system (ROMS): A split-explicit, free-surface, topography-following-coordinate oceanic model. *Ocean Modelling* **9**(4): 347–404. DOI: https://dx.doi.org/10.1016/j.ocemod.2004.08.002.

Silberberger, MJ, Renaud, PE, Espinasse, B, Reiss, H. 2016. Spatial and temporal structure of the meroplankton community in a sub-Arctic shelf system. *Marine Ecology Program Series* **555**: 79–93. DOI: https://dx.doi.org/10.3354/meps11818.

Similä, T, Holst, JC, Christensen, I. 1996. Occurrence and diet of killer whales in Northern Norway: Seasonal patterns relative to the distribution and abundance of Norwegian spring-spawning herring. *Canadian Journal of Fisheries and Aquatic Sciences* **53**(4): 769–779. DOI: https://dx.doi.org/10.1139/f95-253.

Skarðhamar, J, Albretsen, J, Sandvik, AD, Lien, VS, Myksvoll, MS, Johnsen, IA, Asplin, L, Ådlandsvik, B, Halttunen, E, Bjørn, PA. 2018. Modelled salmon lice dispersion and infestation patterns in a sub-arctic fjord. *ICES Journal of Marine Science* **75**(5): 1733–1747. DOI: https://dx.doi.org/10.1093/icesjms/fsy035.

Skarðhamar, J, Slagstad, D, Edvardsen, A. 2007. Plankton distributions related to hydrography and circulation dynamics on a narrow continental shelf off Northern Norway. *Estuarine, Coastal and Shelf Science* **75**(3): 381–392. DOI: https://dx.doi.org/10.1016/j.ecss.2007.05.044.

Skarðhamar, J, Svendsen, H. 2005. Circulation and shelf-ocean interaction off North Norway. *Continental Shelf Research* **25**(12–13): 1541–1560. DOI: https://dx.doi.org/10.1016/j.csr.2005.04.007.

Sørensen, HL, Meire, L, Juul-Pedersen, T, de Stigter, HC, Meysman, FJR, Rysgaard, S, Thamdrup, B, Glud, RN. 2015. Seasonal carbon cycling in a Greenlandic fjord: An integrated pelagic and benthic study. *Marine Ecology Program Series* **539**: 1–17. DDOI: https://dx.doi.org/10.3354/meps11503.

Stübner, EI, Søreide, JE, Reigstad, M, Marquardt, M, Blachowiak-Samolyk, K. 2016. Year-round meroplankton dynamics in high-Arctic Svalbard. *Journal of Plankton Research* **38**(3): 522–536. DOI: https://dx.doi.org/10.1093/plankt/fbv124.

Sundby, S. 1976. *Oseanografiske forhold i området Malangsgrunnen-Fugløybanken-Tromsøflaket*. En oversikt. Fisken og Havet B1. Bergen, Norway: Institute of Marine Research.

Sundby, S. 1984. *Influence of bottom topography on the circulation at the continental shelf off Northern*

Norway. Bergen, Norway: Fiskeridirektoratets Skrifter: Havundersøkelser.

Svensen, C, **Morata, N**, **Reigstad, M**. 2014. Increased degradation of copepod faecal pellets by co-acting dinoflagellates and *Centropages hamatus*. *Marine Ecology Program Series* **516**: 61–70. DOI: https://dx.doi.org/10.3354/meps10976.

Sverdrup, HU. 1953. On conditions for the vernal blooming of phytoplankton. *ICES Journal of Marine Science* **18**(3): 287–295. DOI: https://dx.doi.org/10.1093/icesjms/18.3.287.

Tande, K, **Slagstad, D**. 1992. Regional and interannual variations in biomass and productivity of the marine copepod, *Calanus finmarchicus*, in sub-arctic environments. *Oceanologica Acta* **15**(3): 309–321.

Townsend, DW, **Keller, MD**, **Sieracki, ME**, **Ackleson, SG**. 1992. Spring phytoplankton blooms in the absence of vertical water column stratification. *Nature* **360**(6399): 59–62. DOI: https://dx.doi.org/10.1038/360059a0.

Valiela, I. 2015. *Marine ecological processes*. 3rd ed. Woods Hole, MA: Springer.

Viddi, FA, **Hucke-Gaete, R**, **Torres-Florez, JP**, **Ribeiro, S**. 2010. Spatial and seasonal variability in cetacean distribution in the fjords of northern Patagonia, Chile. *ICES Journal of Marine Science* **67**(5): 959–970. DOI: https://dx.doi.org/10.1093/icesjms/fsp288.

Walker, EZ, **Wiedmann, I**. 2022. Seasonality of suspended and exported Chl *a* and POC and Zooplankton at station KaF, Kaldfjorden (WHALE project). DOI: https://dx.doi.org/10.21335/NMDC-2116003163.

Wassmann, P, **Reigstad, M**, **Øygarden, S**, **Rey, F**. 2000. Seasonal variation in hydrography, nutrients, and suspended biomass in a subarctic fjord: Applying hydrographic features and biological markers to trace water masses and circulation significant for phytoplankton production. *Sarsia* **85**(3): 237–249. DOI: https://dx.doi.org/10.1080/00364827.2000.10414576.

Wassmann, P, **Svendsen, H**, **Keck, A**, **Reigstad, M**. 1996. Selected aspects of the physical oceanography and particle fluxes in fjords of Northern Norway. *Journal of Marine Systems* **8**(1): 53–71. DOI: https://dx.doi.org/10.1016/0924-7963(95)00037-2.

Weslawski, JM, **Kwasniewski, S**, **Wiktor, J**. 1991. Winter in a Svalbard fjord ecosystem. *Arctic* **44**(2): 115–123.

Weydmann, A, **Carstensen, J**, **Goszczko, I**, **Dmoch, K**, **Olszewska, A**, **Kwasniewski, S**. 2014. Shift towards the dominance of boreal species in the Arctic: Interannual and spatial zooplankton variability in the West Spitsbergen Current. *Marine Ecology Program Series* **501**: 41–52. DOI: https://dx.doi.org/10.3354/meps10694.

Wiborg, KF. 1954. Investigations on zooplankton in Norwegian waters and in the Norwegian Sea during 1957–58. Bergen, Norway: Fiskeridirektoratets Skrifter: Havundersøkelser.

Wiedmann, I, **Reigstad, M**, **Marquardt, M**, **Vader, A**, **Gabrielsen, TM**. 2016. Seasonality of vertical flux and sinking particle characteristics in an ice-free high arctic fjord—Different from subarctic fjords? *Journal of Marine Systems* **154**: 192–205. DOI: https://dx.doi.org/10.1016/j.jmarsys.2015.10.003.

Zajączkowski, M, **Nygård, H**, **Hegseth, EN**, **Berge, J**. 2010. Vertical flux of particulate matter in an Arctic fjord: The case of lack of the sea-ice cover in Adventfjorden 2006–2007. *Polar Biology* **33**(2): 223–239. DOI: https://dx.doi.org/10.1007/s00300-009-0699-x.

Zamora-Terol, S, **Saiz, E**. 2013. Effects of food concentration on egg production and feeding rates of the cyclopoid copepod Oithona davisae. *Limnology and Oceanography* **58**(1): 376–387. DOI: https://dx.doi.org/10.4319/lo.2013.58.1.0376.

Zenkevitch, L. 1963. *Biology of the seas of the USSR*. London, UK: George Allen & Unwin Ltd.

ELEMENTA
Science of the Anthropocene

Elem Sci Anth is a peer-reviewed open access journal published by University of California Press.

OPEN ACCESS